

Structure learning for extremal tree models

Sebastian Engelke¹ and Stanislav Volgushev²

¹ Research Center for Statistics, University of Geneva, Boulevard du Pont d'Arve 40,
1205 Geneva, Switzerland.

²Department of Statistical Sciences, University of Toronto, 700 University Ave.,
Toronto, ON M5G 1X6, Canada.

Abstract

Extremal graphical models are sparse statistical models for multivariate extreme events. The underlying graph encodes conditional independencies and enables a visual interpretation of the complex extremal dependence structure. For the important case of tree models, we develop a data-driven methodology for learning the graphical structure. We show that sample versions of the extremal correlation and a new summary statistic, which we call the extremal variogram, can be used as weights for a minimum spanning tree to consistently recover the true underlying tree. Remarkably, this implies that extremal tree models can be learned in a completely non-parametric fashion by using simple summary statistics and without the need to assume discrete distributions, existence of densities, or parametric models for bivariate distributions.

Keywords: Extreme value theory; Domain of attraction; Minimum spanning tree; Multivariate Pareto distribution; Graphical models

1 Introduction

Extreme value theory provides essential statistical tools to quantify the risk of rare events such as floods, heatwaves or financial crises (e.g. Katz et al., 2002; Poon et al., 2004; Engelke et al., 2019). The univariate case is well understood and the generalized extreme value and Pareto distributions describe the distributional tail with only few parameters. In dimension $d \geq 2$, the dependence between large values in the different components of a random vector $\mathbf{X} = (X_1, \dots, X_d)$ can become very complex. Estimating this dependence in higher dimensions is particularly challenging because the number of extreme observations k_n is by definition much smaller than the number n of all samples in a data set. Constructing sparse models for the multivariate dependence between marginal extremes is therefore crucial for obtaining tractable and reliable methods in multivariate extremes; see Engelke and Ivanovs (2021) for a review of recent advances.

One line of research aims at exploiting conditional independence structures (Dawid, 1979) and corresponding graphical models. In the setting of max-stable distributions, which arise as limits of component-wise block maxima of independent copies of \mathbf{X} , Gissibl and Klüppelberg (2018) and Klüppelberg and Lauritzen (2019) study max-linear models on directed acyclic graphs. The distributions considered in there do not have densities, and a general result by Papastathopoulos and Strokorb (2016) shows that there exist no non-trivial density factorization of max-stable distributions on graphical structures.

A different perspective on multivariate extremes is given by threshold exceedances and the resulting class of multivariate Pareto distributions. Such distributions are the only possible limits that can arise from the conditional distribution of \mathbf{X} given that it exceeds a high threshold

(Rootzén and Tajvidi, 2006; Rootzén et al., 2018). For a d -dimensional random vector \mathbf{Y} that follows a multivariate Pareto distribution, Engelke and Hitz (2020) introduce suitable notions of conditional independence and extremal graphical models with respect to a graph G . They further show that these notions are natural as they imply the factorization of the density of \mathbf{Y} through a Hammersley–Clifford type theorem. Extremal graphical models are also related to limits of regularly varying Markov trees studied in Segers (2019) and Asenova et al. (2020).

In most of the above the above work, the graphical structure G is assumed to be known *a priori*. It is either based on expert knowledge in the domain of application or it might be identified with an existing graph, as for instance a river network for discharge measurements. However, often no or insufficient domain knowledge on a prior candidate for a graphical structure is available, and a data-driven approach should be followed in order to detect conditional independence relations and to estimate a sensible graph structure. In this work we discuss structural learning for extreme observations.

An important sub-class of general graphs for which structure learning for extremes turns out to be possible in great generality is given by trees. A tree $T = (V, E)$ with nodes V and edge set E is a connected undirected graph without cycles. Most structure learning approaches for trees are based on the notion of the minimum spanning tree. For a set of symmetric weights $\rho_{ij} > 0$ associated with any pair of nodes $i, j \in V$, $i \neq j$, the latter is defined as the tree structure

$$T_{\text{mst}} = \arg \min_{T=(V,E)} \sum_{(i,j) \in E} \rho_{ij}, \quad (1)$$

that minimizes the sum of distances on that tree. Given the set of weights, there exist greedy algorithms that constructively solve this minimization problem (Kruskal, 1956; Prim, 1957).

The crucial ingredient for this algorithm are the weights ρ_{ij} between the nodes, and for statistical inference it is generally desirable to choose them in such a way that T_{mst} recovers the true underlying tree structure that represents the conditional independence relations. A common approach in graphical modelling is to use the Chow–Liu tree (Chow and Liu, 1968), which is the conditional independence structure that maximizes the likelihood for a given parametric model (cf., Cowell et al., 2006, Chapter 11). This method uses the negative mutual information as edge weights ρ_{ij} in (1), and in general this requires formulating parametric models for the bivariate marginal distributions. In the Gaussian case the weights then simplify to $\rho_{ij} = \log(1 - r_{ij}^2)/2$, where r_{ij} are the correlation coefficients (cf., Drton and Maathuis, 2017).

In this paper we study structure learning for a multivariate Pareto distribution \mathbf{Y} that is an extremal graphical model on a tree T . We show that a function of the extremal correlation χ_{ij} , a widely used coefficient to summarize the strength of extremal dependence between marginals $i, j \in V$ (e.g., Coles et al., 1999), can be used as weights ρ_{ij} in (1) to retrieve the underlying tree structure T as the minimum spanning tree. We further introduce a new summary coefficient for extremal dependence, the extremal variogram Γ_{ij} , which turns out to take a similar role in multivariate extremes as covariances in Gaussian models. More precisely, the extremal variogram of \mathbf{Y} is shown to be an additive tree metric on the tree T and, as a consequence, it can be used as well as weights ρ_{ij} of the minimum spanning tree to recover the true tree structure. Surprisingly, these results are stronger than for non-extremal tree structures, since we do not require any further parametric assumptions or the existence of densities. This phenomenon originates from the homogeneity of multivariate Pareto distributions and particularly nice stochastic representations of extremal tree models.

In practice, when we observe n samples of \mathbf{X} in the domain of attraction of \mathbf{Y} , we rely on estimators of the quantities χ_{ij} and Γ_{ij} to plug into (1). Based on the $k_n < n$ most extreme observations, we use an existing estimator $\hat{\chi}_{ij}$ of extremal correlation and a new empirical estimator of the extremal variogram to show that the extremal tree structure can be estimated consistently in a non-parametric way. For consistent structure estimation, we only require that $k_n/n \rightarrow q \in [0, q^*]$ as $n \rightarrow \infty$, where $q^* > 0$ is an unknown but positive value. This is a much

weaker condition than $k_n/n \rightarrow 0$, which is usually assumed in asymptotic theory of extreme value estimators.

The remaining paper is organized as follows. In Section 2 we revisit the notion of extremal graphical models and extend existing representations to the case where densities may not exist. The extremal variogram is introduced in Section 3 and its properties are discussed in detail. In Section 4 we prove the main results on the consistent recovery of extremal tree structures based on extremal correlations and extremal variograms, both on the population level and using empirical estimates. The simulation studies in Section 5 illustrate the finite sample behavior of our structure estimators and show that extremal variogram based methods typically outperform methods working with the extremal correlation. We apply the new tools in Section 6 to a financial data set of foreign exchange rates. The Appendix and the Supplementary Material contain the proofs and additional illustrations. The methods of this paper are implemented in the R package `graphicalExtremes` (Engelke et al., 2019).

2 Extremal graphical models

2.1 Multivariate Pareto distributions

Multivariate Pareto distributions arise as the limits of high threshold exceedances and are thus natural models for extreme events (cf., Rootzén and Tajvidi, 2006). They can capture both the marginal tail behavior and the multivariate extremal dependence structure between different variables. Similarly to a copula approach, we consider here normalized marginals and refer to Rootzén et al. (2018) for representations with general marginal distributions.

Let $\mathbf{X} = (X_i)_{i \in V}$ be a multivariate random vector with continuous marginal distributions F_i , $i \in V = \{1, \dots, d\}$. Under the assumption of multivariate regular variation (cf., Resnick, 2008) the rescaled tail probabilities of \mathbf{X} converge to the stable tail dependence function

$$\ell(\mathbf{x}) = \lim_{q \rightarrow 0} q^{-1} \mathbb{P}(F(\mathbf{X}) \not\leq 1 - q\mathbf{x}), \quad \mathbf{x} \geq 0, \quad (2)$$

which is a convex and homogeneous function of order one, that is, $\ell(s\mathbf{x}) = s\ell(\mathbf{x})$ for all $s > 0$.

In this case, the exceedances of \mathbf{X} on the marginal scale of standard Pareto distributions converge to a multivariate Pareto distribution

$$\mathbb{P}(\mathbf{Y} \leq \mathbf{x}) = \lim_{q \rightarrow 0} \mathbb{P}\left(\frac{1}{1 - F(\mathbf{X})} \leq \mathbf{x}/q \mid \|F(\mathbf{X})\|_\infty > 1 - q\right) = \frac{\ell(1/\mathbf{x} \wedge \mathbf{1}) - \ell(1/\mathbf{x})}{\ell(\mathbf{1})}, \quad \mathbf{x} \in \mathcal{L},$$

which is supported on the set $\mathcal{L} = \{\mathbf{x} \geq \mathbf{0} : \|\mathbf{x}\|_\infty > 1\}$. We say that the random vector \mathbf{X} is in the max-domain of attraction of the multivariate Pareto distribution $\mathbf{Y} = (Y_i)_{i \in V}$. The latter satisfies the homogeneity property

$$\mathbb{P}(\mathbf{Y} \in tA) = t^{-1} \mathbb{P}(\mathbf{Y} \in A), \quad t \geq 1, \quad (3)$$

where for any Borel subset $A \subset \mathcal{L}$ we define $tA = \{tx : x \in A\}$. This implies that for any $i \in V$ we have $\mathbb{P}(Y_i > x \mid Y_i > 1) = 1/x$ for $x > 1$. The homogeneity in (3) can also be taken as the defining property for multivariate Pareto distributions.

Remark 1 *To any multivariate Pareto distribution \mathbf{Y} we can associate a max-stable distribution \mathbf{Z} by*

$$\mathbb{P}(\mathbf{Z} \leq \mathbf{z}) = \exp\{-\ell(1/\mathbf{z})\}, \quad \mathbf{z} \geq 0.$$

From the definition of the stable tail dependence function in (2) it follows that the margins Z_i , $i \in V$, are standard Fréchet distributed, that is, $\mathbb{P}(Z_i \leq z) = \exp(-1/z)$, $z \geq 0$.

2.2 Extremal Markov structures

Since the support \mathcal{L} of multivariate Pareto distributions is not a product space, the definition of conditional independence is non-standard and relies on certain restricted random vectors derived from \mathbf{Y} . For any $m \in V$, we consider the random vector \mathbf{Y}^m defined as \mathbf{Y} conditioned on the event that $\{Y_m > 1\}$, which has support on the space $\mathcal{L}^m = \{\mathbf{x} \in \mathcal{L} : x_m > 1\}$. We further define the extremal function relative to coordinate m as the d -dimensional, non-negative random vector \mathbf{W}^m with $W_m^m = 1$ almost surely that satisfies the stochastic representation

$$\mathbf{Y}^m \stackrel{(d)}{=} P\mathbf{W}^m, \quad (4)$$

where P is a standard Pareto random variable, $\mathbb{P}(P \leq x) = 1 - 1/x$, $x \geq 1$, which is independent \mathbf{W}^m . Conversely, the set of the d extremal functions $\mathbf{W}^1, \dots, \mathbf{W}^d$ uniquely defines the multivariate Pareto distribution.

Example 1 *In the case $d = 2$, due to homogeneity, the bivariate Pareto distribution $\mathbf{Y} = (Y_1, Y_2)$ can essentially be characterized by a univariate distribution. Indeed, for any positive random variable W_2^1 with $\mathbb{E}W_2^1 \leq 1$, the random vector $\mathbf{W}^1 = (1, W_2^1)$ is the extremal function relative to the first coordinate of a unique bivariate Pareto distribution \mathbf{Y} . The extremal function relative to the second coordinate $\mathbf{W}^2 = (W_1^2, 1)$ is obtained through a change of measure as*

$$\mathbb{P}(W_1^2 \leq z, W_1^2 > 0) = \mathbb{E}(\mathbf{1}\{1/W_2^1 \leq z\}W_2^1), \quad z > 0, \quad (5)$$

which implies that $\mathbb{E}(W_2^1) = 1 - \mathbb{P}(W_1^2 = 0) \leq 1$.

With this notation we can state a definition of conditional independence for multivariate Pareto distributions that is more general than the one in (Engelke and Hitz, 2020), since we do not assume existence of densities.

Definition 1 *For disjoint subsets $A, B, C \subset V = \{1, \dots, d\}$, we say that \mathbf{Y}_A is conditionally independent of \mathbf{Y}_C given \mathbf{Y}_B if*

$$\forall m \in \{1, \dots, d\} : \quad \mathbf{Y}_A^m \perp\!\!\!\perp \mathbf{Y}_C^m \mid \mathbf{Y}_B^m. \quad (6)$$

In this case we write $\mathbf{Y}_A \perp_e \mathbf{Y}_C \mid \mathbf{Y}_B$.

We view the index set V as a set of nodes of a graph $G = (V, E)$, with connections given by a set of edges $E \subset V \times V$ of pairs of distinct nodes. The graph is called undirected if for two nodes $i, j \in V$, $(i, j) \in E$ if and only if $(j, i) \in E$. For notational convenience, for undirected graphs we sometimes represent edges as unordered pairs $\{i, j\} \in E$. When counting the number of edges, we count $\{i, j\} \in E$ such that each edge is considered only once. For disjoint subsets $A, B, C \subset V$, B is said to separate A and C in G if every path from A to C contains at least one node in B .

The notion of an extremal graphical model is then naturally defined as a multivariate Pareto distribution that satisfies the global Markov property on the graph G with respect to the conditional independence relation \perp_e , that is, for any disjoint subsets $A, B, C \subset V$ such that B separates A from C in G ,

$$\mathbf{Y}_A \perp_e \mathbf{Y}_C \mid \mathbf{Y}_B. \quad (7)$$

In the case of a decomposable graph G and if \mathbf{Y} possesses a positive and continuous density $f_{\mathbf{Y}}$, Engelke and Hitz (2020) show that this density factorizes into lower-dimensional densities, and that the graph G is necessarily connected. If \mathbf{Y} does not have a density, then the extremal graph can be disconnected and the connected components are mutually independent of each other (Engelke and Hitz, 2020, see Kirstin Strokorb's discussion contribution). Note that we require the global Markov property in the definition of extremal graphical models as opposed to the pairwise Markov property used in Engelke and Hitz (2020). Both properties are equivalent in the case of positive, continuous densities, but in general, the former implies the latter but not the other way around (see Lauritzen, 1996, Chapter 3).

2.3 Extremal tree models

An important example of a sparse graph structure is a tree. A tree $T = (V, E)$ is a connected undirected graph without cycles and thus $|E| = |V| - 1$. Equivalently, a tree is a graph with a unique path between any two nodes. If \mathbf{Y} is an extremal graphical model satisfying the global Markov property (7) with respect to a tree T , we obtain a simple stochastic representation of \mathbf{Y}^m . To this end, we define a new, directed tree $T^m = (V, E^m)$ rooted at an arbitrary but fixed node $m \in V$. The edge set E^m consist of all edges $e \in E$ of the tree T pointing away from node m . For the resulting directed tree we define a set $\{W_e : e \in E^m\}$ of independent random variables, where for $e = (i, j)$, the distribution of $W_e = W_j^i$ is the extremal function of \mathbf{Y} at coordinate j , relative to coordinate i .

The following result generalizes Proposition 2 in Engelke and Hitz (2020) to extremal tree models with arbitrary edge distributions. It also formally establishes the link of the conditional independence in Definition 1 to the limiting tail trees in Segers (2019).

Proposition 1 *Let \mathbf{Y} be a multivariate Pareto distribution that is an extremal graphical model on the tree $T = (V, E)$. Let P be a standard Pareto distribution, independent of $\{W_e : e \in E^m\}$. Then we have the joint stochastic representation for \mathbf{Y}^m on \mathcal{L}^m*

$$Y_i^m \stackrel{(d)}{=} \begin{cases} P, & \text{for } i = m, \\ P \times \prod_{e \in \text{ph}(mi)} W_e, & \text{for } i \in V \setminus \{m\}, \end{cases} \quad (8)$$

where $\text{ph}(mi)$ denotes the set of edges on the unique path from node m to node i on the tree T^m ; see Figure 1 for an example with $m = 2$.

Conversely, for any set of independent random variables $\{W_i^j, W_j^i; \{i, j\} \in E\}$, where W_i^j and W_j^i satisfy the duality (5), the construction (8) defines a consistent family of extremal functions $\mathbf{W}^1, \dots, \mathbf{W}^d$ that correspond to a unique d -dimensional Pareto distribution \mathbf{Y} which is an extremal graphical model on T .

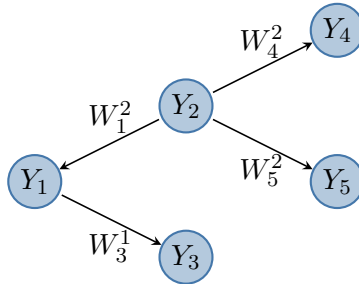


Figure 1: A tree T^2 rooted at node $m = 2$ with the extremal functions on the edges.

Remark 2 *It is remarkable that for an extremal tree model \mathbf{Y} , the distribution of its extremal functions, and therefore also of the multivariate Pareto distribution itself, is characterized by the set of univariate random variables $\{W_i^j, W_j^i; \{i, j\} \in E\}$. This indicates that the probabilistic structure is simpler than in the non-extremal case, where in general both univariate and bivariate distributions are needed to describe a tree graphical model.*

3 The extremal variogram

Covariance matrices play a central role in structure learning for Gaussian graphical models due to their connection to conditional independence properties. In multivariate extreme value theory, several summary statistics have been developed to measure the strength of dependence

between the extremes of different variables. The most popular one is the extremal correlation, which for $i, j \in V$ is defined as

$$\chi_{ij} := \lim_{q \rightarrow 0} \chi_{ij}(q) := \lim_{q \rightarrow 0} \mathbb{P} \{F_i(X_i) > 1 - q \mid F_j(X_j) > 1 - q\}, \quad (9)$$

whenever the limit exists. It ranges between 0 and 1 where the boundary cases are asymptotic independence and complete extremal dependence, respectively (cf., Coles et al., 1999; Schlather and Tawn, 2003). In particular, if \mathbf{X} is in the max-domain of attraction of the multivariate Pareto distribution \mathbf{Y} , then the extremal correlation always exists and $\chi_{ij} = \mathbb{P}(Y_i > 1 \mid Y_j > 1)$. There are many other coefficients for extremal dependence in the literature, including the madogram (Cooley et al., 2006) and a coefficient defined on the spectral measure introduced in Larsson and Resnick (2012) and used for dimension reduction in Cooley and Thibaud (2019) and Fomichov and Ivanovs (2020).

While designed as summaries for extremal dependence, none of these coefficients has an obvious relation to conditional independence for multivariate Pareto distributions or density factorization in extremal graphical models of Engelke and Hitz (2020). In this section we define a new coefficient that will turn out to take a similar role in multivariate extremes as covariances in non-extremal models.

3.1 Limiting extremal variogram

The variogram is a well-known object in geostatistics that measures the degree of spatial dependence of a random field (cf., Chilès and Delfiner, 2012; Wackernagel, 2013). It is similar to a covariance function, but instead of positive definiteness, a variogram is conditionally negative definite; for details, see for instance Engelke and Hitz (2020, Appendix B). For Brown–Resnick processes, the seminal work of Kabluchko et al. (2009) has shown that negative definite functions play a crucial role in spatial extreme value theory. We define a variogram for general multivariate Pareto distributions.

Definition 2 *For a multivariate Pareto distribution \mathbf{Y} we define the extremal variogram rooted at node $m \in V$ as the matrix $\Gamma^{(m)}$ with entries*

$$\Gamma_{ij}^{(m)} = \text{Var} \{ \log Y_i^m - \log Y_j^m \}, \quad i, j \in V, \quad (10)$$

whenever the right-hand side exists in $[0, \infty)$.

We can interpret the $\Gamma_{ij}^{(m)}$ as a distance between the variables Y_i^m and Y_j^m that is large if they are weakly extremal dependent and *vice versa*.

Proposition 2 *Let \mathbf{Y} be a multivariate Pareto distribution.*

- (i) *For $m \in V$, we can express the extremal variogram in terms of the extremal function relative to coordinate m ,*

$$\Gamma_{ij}^{(m)} = \text{Var} \{ \log W_i^m - \log W_j^m \}, \quad i, j \in V.$$

- (ii) *For $m \in V$, the matrix $\Gamma^{(m)}$ is a variogram matrix, that is, it is conditionally negative definite.*
- (iii) *Let \mathbf{Y}_n be a sequence of multivariate Pareto distributions with extremal coefficients satisfying $\chi_{im}(n) \rightarrow 0$ as $n \rightarrow \infty$ for some $i, m \in V$. Then the extremal variograms satisfy $\Gamma_{im}^{(m)}(n) \rightarrow \infty$.*

Part (iii) in the above proposition underlines the interpretation of the extremal variogram. When the variables become asymptotically independent, then the extremal variogram grows and eventually diverges to $+\infty$. Note that the inverse statement is not true in general, since there are cases where $\Gamma_{im}^{(m)} = \infty$ but $\chi_{im} > 0$. We proceed with several examples where the extremal variogram can be computed explicitly. Figure 2 shows the extremal variogram values for these models as a function of the corresponding extremal correlation.

Example 2 *The extremal logistic distribution with parameter $\theta \in (0, 1)$ can be defined through its extremal functions (see Dombry et al., 2016)*

$$\mathbf{W}^m = (U_1/U_m, \dots, U_d/U_m),$$

where U_1, \dots, U_d are independent and U_i , $i \neq m$ follow Fréchet($1/\theta, G(1-\theta)^{-1}$) distributions, and $(G(1-\theta)U_m)^{-1/\theta}$ follows a Gamma($1-\theta, 1$) distribution; here $G(x)$ is the Gamma function evaluated at $x \geq 0$. It turns out that for the logistic model we have

$$\Gamma_{ij}^{(m)} = \begin{cases} \pi^2\theta^2/3, & \text{if } i, j \neq m, \\ \theta^2\{\psi^{(1)}(1-\theta) + \pi^2/6\}, & \text{if } i = m, j \neq m, \end{cases}$$

where $\psi^{(1)}$ is the trigamma function defined as the second derivative of the logarithm of the gamma function.

The proof of this representation of the extremal variogram in the logistic model can be found in the Supplementary Material S.5.

Example 3 *The extremal Dirichlet distributions with parameters $\alpha_1, \dots, \alpha_d$ (cf., Coles and Tawn, 1991) has extremal functions*

$$\mathbf{W}^m = (U_1/U_m, \dots, U_d/U_m),$$

where U_1, \dots, U_d are independent and U_i , $i \neq m$ follow Gamma($\alpha_i, 1/\alpha_i$) distributions, and U_m follows a Gamma($\alpha_m + 1, 1/\alpha_m$) distribution. By straight-forward calculations,

$$\Gamma_{ij}^{(m)} = \begin{cases} \psi^{(1)}(\alpha_i) + \psi^{(1)}(\alpha_j), & \text{if } i, j \neq m, \\ \psi^{(1)}(\alpha_m + 1) + \psi^{(1)}(\alpha_j), & \text{if } i = m, j \neq m, \end{cases}$$

with $\psi^{(1)}$ denoting the trigamma function as in Example 2.

For the class of Hüsler–Reiss distributions the extremal variogram turns out to be very natural.

Example 4 *The Hüsler–Reiss distribution is parameterized by a variogram matrix $\Gamma \in \mathbb{R}^{d \times d}$; see (Engelke and Hitz, 2020) for details. For any d -variate centered normal random vector \mathbf{U} with variogram matrix Γ , the extremal function relative to coordinate $m \in V$ can be represented as*

$$\mathbf{W}^m = \exp\{\mathbf{U} - U_m - \Gamma_{\cdot m}/2\}, \quad (11)$$

see Dombry et al. (2016, Prop. 4). The extremal variogram $\Gamma^{(m)}$ for any $m \in V$ is then equal to the variogram matrix Γ from the definition of the Hüsler–Reiss distributions, and, in particular, it is independent of the root node,

$$\Gamma_{ij} = \Gamma_{ij}^{(1)} = \dots = \Gamma_{ij}^{(d)}, \quad i, j \in V.$$

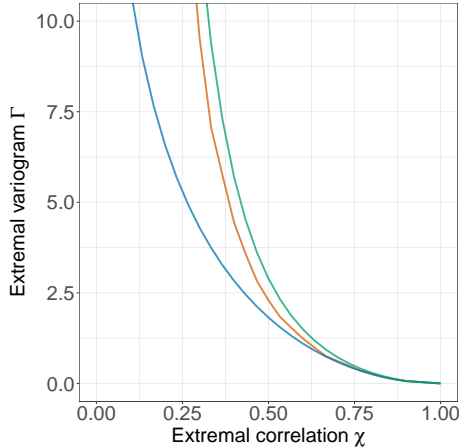


Figure 2: Values of the extremal variogram $\Gamma_{12}^{(1)}$ as a function of the extremal correlation χ_{12} for the bivariate Hüsler–Reiss (blue), symmetric Dirichlet (orange) and logistic (green) models. Note that in all three cases we have that $W_1^2 \stackrel{(d)}{=} W_2^2$ and therefore $\Gamma_{12}^{(1)} = \Gamma_{12}^{(2)}$.

3.2 Pre-asymptotic extremal variogram

Similar to the extremal correlation in (9) we can define the extremal variogram as the limit of pre-asymptotic versions.

Definition 3 For a multivariate distribution \mathbf{X} with continuous marginal distributions we define the pre-asymptotic extremal variogram at level $q \in (0, 1)$ rooted at node $m \in V$ as the matrix $\Gamma^{(m)}(q)$ with entries

$$\Gamma_{ij}^{(m)}(q) = \text{Var} [\log\{1 - F_i(X_i)\} - \log\{1 - F_j(X_j)\} \mid F_m(X_m) > 1 - q], \quad i, j \in V,$$

whenever right-hand side exists.

Note that the terms $-\log\{1 - F_i(X_i)\}$, $i \in V$, transform the margins to unit exponential distributions in order to match Definition 2. Next we provide conditions which ensure the convergence $\Gamma_{ij}^{(m)}(q) \rightarrow \Gamma_{ij}^{(m)}$ as $q \rightarrow 0$. To state the assumption, we introduce the following notation: for a vector $\mathbf{x} \in \mathbb{R}^d$ and $I \subset \{1, \dots, d\}$, let \mathbf{x}_I denote a vector in $\mathbb{R}^{|I|}$ with entries $x_j, j \in I$. For a distribution function F of a d -dimensional random vector \mathbf{X} define F_I as the distribution function of the corresponding random vector \mathbf{X}_I and let ℓ_I denote the limit obtained in relation (2) when $F, \mathbf{X}, \mathbf{x}$ are replaced by $F_I, \mathbf{X}_I, \mathbf{x}_I$.

(B) We have for some $\xi > 0$ and any $I \subset V$ with $|I| \in \{2, 3\}$

$$\sup_{\mathbf{x} \in [0,1]^{|I|}} \left| q^{-1} \mathbb{P}(F_I(\mathbf{X}_I) \not\leq 1 - q\mathbf{x}) - \ell_I(\mathbf{x}) \right| = O(q^\xi) \quad (q \rightarrow 0). \quad (12)$$

(T) There exists a $\gamma > 0$ such that for any $i, m \in V$ the extremal function satisfies

$$\mathbb{E}(W_i^m)^{-\gamma} < \infty. \quad (13)$$

Assumption (B) is a strengthening of (2) as it imposes that convergence to the limit should take place uniformly and at a certain rate. It is in spirit of typical second order conditions which are fairly standard in the literature; see for instance Einmahl et al. (2012) and Fougères et al. (2015) among many others. Condition (T) is a mild assumption on the extremal functions W_i^m , which holds for all examples considered in the previous section. This condition prevents the distribution of W_i^m from putting too much mass close to zero.

Proposition 3 *Under conditions (B), (T) we have for any $m, i, j \in V$*

$$\Gamma_{ij}^{(m)}(q) \rightarrow \Gamma_{ij}^{(m)} \quad (q \rightarrow 0).$$

We note that condition (T) already implies that $\Gamma_{ij}^{(m)} \in [0, \infty)$ for any i, j , so the convergence above is always to a finite limit.

4 Structure learning for extremal tree models

4.1 Extremal tree models

Extremal graphical models where the underlying graph is a tree were considered as a sparse statistical model in Engelke and Hitz (2020). For the class of Hüsler–Reiss distributions (a parametric sub-class of multivariate Pareto distributions) they proposed to use a censored maximum-likelihood tree where the edge weights are essentially given by the negative maximized bivariate log-likelihoods. This approach has two disadvantages. First, in higher dimensions d it may become prohibitively costly to compute d^2 censored likelihood optimizations, and second, a set of parametric bivariate models has to be chosen in advance.

Ideally, one would like to have summary statistics, similar to the correlation coefficients r_{ij} in the Gaussian case, that can be estimated empirically and that guarantee to recover the true underlying tree structure when used as edge weights. The extremal variogram defined in Section 3 turns out to be a so-called tree metric, and as such a natural quantity to infer the conditional independence structure in extremal tree models. We underline that the extremal variogram $\Gamma^{(m)}$ is defined for arbitrary multivariate Pareto distributions and in the case of the Hüsler–Reiss distribution it coincides with the parameter matrix.

Proposition 4 *Let \mathbf{Y} be an extremal graphical model with respect to the tree $T = (V, E)$ and suppose that the extremal variogram matrix $\Gamma^{(m)}$ exists for all $m \in V$. Then we have that*

$$\Gamma_{ij}^{(m)} = \sum_{(s,t) \in \text{ph}(ij)} \Gamma_{st}^{(m)}. \quad (14)$$

In other words, for any $m \in V$, the extremal variogram matrix $\Gamma^{(m)}$ defines an additive tree metric.

Corollary 1 *Let \mathbf{Y} be an extremal graphical model with respect to the tree $T = (V, E)$. Suppose that the extremal variogram matrix $\Gamma^{(m)}$ exists for all $m \in V$ and that $\mathbb{P}(Y_i \neq Y_j) > 0$ for all $i, j \in V, i \neq j$ (or equivalently, $\Gamma_{ij}^{(m)} > 0$). For any $m \in V$, the minimum spanning tree with $\rho_{ij} = \Gamma_{ij}^{(m)}$ is unique and satisfies*

$$T_{\text{mst}} = T.$$

For extremal tree models, Corollary 1 shows that independently of any distributional assumption, the extremal variogram contains the conditional independence structure of the tree T . This result is quite surprising, since it is stronger than what is known in the classical, non-extremal theory of trees. Indeed, as discussed in the introduction, for Gaussian graphical models, a analogous result holds for a minimum spanning tree with weights $\rho_{ij} = \log(1 - r_{ij}^2)/2$ for r_{ij} denoting the correlation between the i th and j th component of the Gaussian random vector under consideration. The assumption of Gaussianity is crucial and the result no longer holds outside this specific parametric class.

Beyond the world of Gaussian graphical models, there exists some literature on the non-parametric estimation of graphical models on tree structures, see Chow and Liu (1968) for an early contribution and Drton and Maathuis (2017, Section 3.1) for an overview. However, one

either needs to assume discrete distributions (Chow and Liu, 1968) or the existence of densities (Liu et al., 2011; Lafferty et al., 2012), and non-parametric density estimation is required in the latter case. To the best of our knowledge, multivariate Pareto distributions are the first example for a non-parametric sub-class of multivariate distributions where tree dependence structures can be learned using simple moment-based summary statistics without additional parametric assumptions. It is also remarkable that there is no need to assume the existence of densities and that the distributions we consider can simultaneously have continuous and discrete components.

The reason why such a strong result can hold can be explained by the homogeneity of the multivariate Pareto distribution \mathbf{Y} . For trees, all cliques contain two nodes and therefore the density $f_{\mathbf{Y}}$ factorizes into bivariate Pareto densities. Because of the homogeneity, such a bivariate density can be decomposed into independent radial and angular parts; see Example 1. Bivariate Pareto distributions only differ in terms of the angular distribution, whose support is a one-dimensional sphere. Consequently, an extremal tree model in d dimensions can essentially be reduced to $d - 1$ univariate angular distributions; see also Proposition 1. This provides an intuitive explanation why the result in Corollary 1 can hold.

We can go further and show that a linear combination of the matrices $\Gamma^{(m)}$, $m \in V$, which are possibly different from each other, still induces the true tree as the minimum spanning tree.

Corollary 2 *Under the same assumptions as in Corollary 1, the minimum spanning tree with distances*

$$\rho_{ij} = \sum_{m=1}^d w_m \Gamma_{ij}^{(m)}$$

given by a linear combination of the extremal variograms rooted at different nodes with coefficients $w_m \geq 0$, $m \in V$, $\max_{m \in V} w_m > 0$, is unique and satisfies $T_{\text{mst}} = T$.

The extremal correlation coefficients χ_{ij} do not form a tree metric, that is, they are not additive according to the tree structure as the extremal variogram in (23). It is therefore a non-trivial question whether these coefficients can also be used as weights in a minimum spanning tree to infer the underlying conditional independence structure. Interestingly, the next result gives an affirmative answer.

Proposition 5 *Let \mathbf{Y} be a multivariate Pareto distribution factorizing on the tree $T = (V, E)$, such that $Y_i \neq Y_j$ for all $i, j \in V$, $i \neq j$ (or equivalently, $\chi_{ij} \neq 1$). The minimum spanning tree corresponding to distances $\rho_{ij} = -\log(\chi_{ij})$ is unique and satisfies*

$$T_{\text{mst}} = T.$$

Remark 3 *Both the extremal variogram $\Gamma_{ij}^{(m)}$ and the extremal correlation χ_{ij} contain the information on conditional independence structure for extremal tree models. When their sample versions are used (see Section 4.2), the probability of correctly identifying the underlying tree may differ; see Section 5. The extremal correlation can be used for any model, while the extremal variogram does not exist if \mathbf{Y} has mass on lower-dimensional sub-faces of \mathcal{L} .*

4.2 Estimation

Throughout this section assume that we observe independent copies $\mathbf{X}_1, \dots, \mathbf{X}_n$ of the d -dimensional random vector \mathbf{X} , which is in the max-domain of attraction of a multivariate Pareto distribution \mathbf{Y} , an extremal graphical model on the tree T according to (7). Our aim is to estimate T from the observations $\mathbf{X}_1, \dots, \mathbf{X}_n$. Motivated by Proposition 5 and Corollaries 1, 2 we propose to achieve this through a two-step procedure. We first construct estimators for the quantities χ_{ij} and $\Gamma_{ij}^{(m)}$, and then compute the minimal spanning trees corresponding to those estimators.

The empirical estimator for χ_{ij} is defined as

$$\hat{\chi}_{ij} := \frac{n}{k} \sum_{t=1}^n \mathbf{1}\{\tilde{F}_i(X_{ti}) > 1 - k/n, \tilde{F}_j(X_{tj}) > 1 - k/n\},$$

where $k = k_n$ is an intermediate sequence and \tilde{F}_i denotes the empirical distribution function of X_{1i}, \dots, X_{ni} . Standard arguments imply that under (2) and provided that $k \rightarrow \infty$, $k/n \rightarrow q \in [0, 1]$ we have for any $i, j \in V$

$$\hat{\chi}_{ij} = \chi_{ij}(q) + o_{\mathbb{P}}(1), \quad (15)$$

where $\chi_{ij}(q)$ is defined in (9) and $\chi_{ij}(0) := \chi_{ij}$. In particular, if $q = 0$ then $\hat{\chi}_{ij}$ is a consistent estimator of χ_{ij} .

The extremal variogram matrix $\Gamma^{(m)}$ for the sample \mathbf{X}_t , $t = 1, \dots, n$, is estimated by

$$\hat{\Gamma}_{ij}^{(m)} := \widehat{\text{Var}}\left(\log(1 - \tilde{F}_i(X_{ti})) - \log(1 - \tilde{F}_j(X_{tj})) : \tilde{F}_m(X_{tm}) \geq 1 - k/n\right),$$

where $\widehat{\text{Var}}$ denotes the sample variance. Under the assumption $k/n \rightarrow q \in [0, 1]$ and mild conditions on the underlying data generation, this estimator can be shown to be consistent for the pre-asymptotic version $\Gamma_{ij}^{(m)}(q)$ as introduced in Definition 3.

Theorem 1 *Let assumptions (B), (T) hold and assume that $k \geq n^\theta$ for some $\theta > 0$ and that $k/n \rightarrow q \in [0, 1]$. Then we have for any $m, i, j \in V$*

$$\hat{\Gamma}_{ij}^{(m)} = \Gamma_{ij}^{(m)}(q) + o_{\mathbb{P}}(1),$$

where $\Gamma_{ij}^{(m)}(0) := \Gamma_{ij}^{(m)}$.

The proof of this result turns out to be surprisingly technical, details are given in the Supplementary Material S.7.2. The main challenge arises from the fact that in the definition of $\Gamma_{ij}^{(m)}$ only the observations in component m are extreme while observations in other components may also be non-extreme. This is different from the setting that is typically considered in asymptotically dependent extreme value theory.

Remark 4 *By choosing $q = 0$, the above theorem implies consistency of the empirical extremal variogram $\hat{\Gamma}^{(m)}$. This result is of independent interest, since it is the first proof of consistency of the moment estimator*

$$\hat{\Sigma}_{ij}^{(m)} = \frac{1}{2} \{\hat{\Gamma}_{im}^{(m)} + \hat{\Gamma}_{jm}^{(m)} - \hat{\Gamma}_{im}^{(m)}\}_{i,j \neq m} \in \mathbb{R}^{(d-1) \times (d-1)},$$

which was introduced in Engelke et al. (2015) as an estimator for the parameters of the Hüsler-Reiss distribution.

Remark 5 *The assumption that the data $\mathbf{X}_1, \dots, \mathbf{X}_n$ are independent was only made to keep the presentation simple. The consistency result in Theorem 1 continues to hold under a high-level assumption that allows for temporal dependence and is spelled out in detail in the Supplementary Material at the beginning of Section S.7.2.*

Now we have all results that are needed for consistent estimation of the underlying tree structure. Given a general distance ρ with estimator $\hat{\rho}$ on pairs $(i, j) \in V \times V$, we consider plug-in procedures of the form

$$\hat{T}_\rho := \arg \min_{T=(V,E)} \sum_{(i,j) \in E} \hat{\rho}_{ij}, \quad (16)$$

with three cases of particular interest given by

$$\hat{\rho}_{ij} = -\log(\hat{\chi}_{ij}), \quad \hat{\rho}_{ij} = \hat{\Gamma}_{i,j}^{(m)}, \quad \hat{\rho}_{ij} = \sum_{m=1}^d w_m \hat{\Gamma}_{ij}^{(m)},$$

resulting in the estimators $\hat{T}_\chi, \hat{T}_\Gamma^{(m)}, \hat{T}_\Gamma^w$, respectively. The special case of $w_1 = \dots = w_d = 1/d$ is denoted by \hat{T}_Γ . We solve the minimum spanning tree problem (16) by Prim's algorithm (Prim, 1957), which is guaranteed to find an optimizer of problem (16).

Theorem 2 *Assume that \mathbf{Y} is a multivariate Pareto distribution that factorizes over the tree T . If (2) holds and if $k \rightarrow \infty$ then there exists $q^* > 0$ such that under the additional assumption $k/n \rightarrow q \in [0, q^*]$*

$$\mathbb{P}(\hat{T}_\chi = T) \rightarrow 1.$$

If assumptions (B), (T) hold and if $k \geq n^\theta$ for some $\theta > 0$ then for any $m \in V$ there exists $q_m^ > 0$ such that for $k/n \rightarrow q \in [0, q_m^*]$ we have*

$$\mathbb{P}(\hat{T}_\Gamma^{(m)} = T) \rightarrow 1.$$

The same is true for \hat{T}_Γ^w provided the weights w_m satisfy $w_m \geq 0, \max_m w_m > 0$.

Remark 6 *At first glance it might seem surprising that the tree structure can be estimated consistently even when k_n/n does not converge to zero. The latter would be a classical minimal assumption in extreme value theory and would be required for consistent estimation of χ_{ij} or $\Gamma_{ij}^{(m)}$. We explain the intuition behind this result for the extremal correlation, the arguments for the extremal variogram are exactly the same. The key insight is that even biased estimators of $\chi_{ij}(q)$ can lead to the correct minimal spanning tree since all we need is*

$$\sum_{(i,j) \in E'} -\log \chi_{ij}(q) > \sum_{(i,j) \in E} -\log \chi_{ij}(q)$$

for all trees $T' = (V, E') \neq T$, where T denotes the true underlying tree. Multivariate regular variation (2) implies that $\chi_{ij}(q) \rightarrow \chi_{ij}$ as $q \rightarrow 0$ for all i, j , so the above inequality is satisfied for all $q < q_0$ for some $q_0 > 0$. Since in addition $\hat{\chi}_{ij} = \chi_{ij}(k/n) + o_{\mathbb{P}}(1)$ under the assumption $k \rightarrow \infty$, consistency follows.

Theorem 2 shows that the proposed procedures are able to consistently recover the tree structure under rather weak assumptions on the sequence $k = k_n$. It is natural to wonder which choices of k correspond to higher probabilities of recovering the tree structure consistently. Here we provide some indicative discussion of this issue for minimal spanning trees based on χ_{ij} without going into technical details. Standard results from empirical process theory show that under mild assumptions and for $k/n \rightarrow q \in [0, 1]$ all $\sqrt{k}(\hat{\chi}_{ij} - \chi_{ij}(k/n))$ converge jointly to a multivariate normal distribution with covariance matrix Σ_q . The latter satisfies $\Sigma_q \rightarrow \Sigma_0$ for $q \rightarrow 0$. Combined with the delta method this implies that for any tree $T' = (V, E') \neq T$

$$\sum_{(i,j) \in E'} \hat{\rho}_{ij} - \sum_{(i,j) \in E} \hat{\rho}_{ij} = \Delta_{k,n} + \frac{1}{\sqrt{k}} Z_{k,n} := \sum_{(i,j) \in E'} \rho_{ij}(k/n) - \sum_{(i,j) \in E} \rho_{ij}(k/n) + \frac{1}{\sqrt{k}} Z_{k,n}$$

where $\rho_{ij}(k/n) := -\log \chi_{ij}(k/n)$ and $\hat{\rho}_{ij} := -\log \hat{\chi}_{ij}$, and $Z_{k,n}$ is a weighted linear combination of differences $\sqrt{k}(\hat{\chi}_{ij} - \chi_{ij}(k/n))$ and thus approximately centered normal with variance σ_q^2 . The probability that the sum over estimated distances on T' is shorter than the sum over true tree T is given by $\mathbb{P}(-Z_{k,n} > \sqrt{k}\Delta_{k,n})$. Under the assumptions for asymptotic normality of $\hat{\chi}_{ij}$, $\Delta_{k,n}$ converges to $\Delta(q) := \sum_{(i,j) \in E'} \rho_{ij}(q) - \sum_{(i,j) \in E} \rho_{ij}(q)$. Combining all of the above

approximations we find $\mathbb{P}(-Z_{k,n} > \sqrt{k}\Delta_{k,n}) \approx \mathbb{P}(\sigma_q \mathcal{N}(0, 1) > \sqrt{n}\sqrt{q}\Delta(q))$. Since $\sigma_q \rightarrow \sigma_0 > 0$ and $\Delta(q) \rightarrow \Delta(0) > 0$ as $q \rightarrow 0$, it is easy to see that there exists $q_0 > 0$ such that $\sqrt{q}\Delta(q)/\sigma_q < \sqrt{q_0}\Delta(q_0)/\sigma_{q_0}$ for all $q < q_0$, and thus the probability of selecting T' instead of the true tree T starts to increase as the limit of k/n decreases after q_0 . This suggests that an optimal value for k in terms of maximizing the probability of estimating the true tree would satisfy $k/n \rightarrow \tilde{q}$ for some $\tilde{q} > 0$. Turning the above arguments into a formal proof would require many technicalities which are beyond the scope of the present paper, but the intuition obtained here is also confirmed in the simulations in Section 5.

5 Simulations

The minimum spanning trees based on the empirical versions of the extremal variogram and extremal correlation both recover asymptotically the underlying extremal tree structure. In this section we study the finite sample behavior of the different tree estimators on simulated data. The results and figures of Sections 5 and 6 can be reproduced with the code at https://github.com/sebastian-engelke/extremal_tree_learning.

Let $T = (V, E)$ be a random tree structure that is generated by sampling uniformly $d - 1$ edges and adding these to the empty graph under the constraint to avoid circles. Throughout the whole section, we simulate n samples $\mathbf{X}_1, \dots, \mathbf{X}_n$ from a random vector \mathbf{X} in the domain of attraction of a multivariate Pareto distribution \mathbf{Y} that is an extremal graphical model on the tree T in dimension $d = |V|$. As random vector \mathbf{X} we take the corresponding max-stable distribution, which is indeed in the domain of attraction of \mathbf{Y} in the sense of (2); see also Remark 1. In order to perturb the samples, a common way is to add lighter tailed noise (e.g., Einmahl et al., 2016). More precisely,

$$\mathbf{X}_i = \mathbf{Z}_i + \varepsilon_i, \quad \varepsilon_i \perp\!\!\!\perp \mathbf{Z}_i, \quad i = 1, \dots, n, \quad (17)$$

where \mathbf{Z}_i is a max-stable random vector with standard Fréchet margins associated to \mathbf{Y} , and ε_i is a lighter-tailed noise vector which is independent of \mathbf{Z}_i . We consider two scenarios for the noise distribution, where in both cases the marginal distribution is transformed to a Fréchet distribution with $\mathbb{P}(\varepsilon_{ij} \leq x) = \exp(-1/x^2)$, $x \geq 0$, $j \in V$.

(N1) The noise vector ε_i has independent entries.

(N2) The noise vector ε_i in (17) is generated from an extremal tree model on a fixed tree T_{noise} that is generally different from the true tree T .

Since the marginals of the noise vector have lighter tails, the limit of \mathbf{X}_i in (2) is not altered by ε_i . The main difference between the two noise mechanisms lies in the type of bias they introduce for large k , and we observe that this has an interesting impact on the recovery of the tree structure underlying \mathbf{Y} .

We consider two different parametric classes of distributions for \mathbf{Y} .

(M1) The Hüsler–Reiss tree model is a multivariate Pareto distribution that factorizes on $T = (V, E)$, where each bivariate distribution (Y_i, Y_j) for $(i, j) \in E$ is Hüsler–Reiss with parameter $\Gamma_{ij} > 0$; see Example 4. The joint distribution is then also Hüsler–Reiss with parameter matrix Γ induced by the tree structure through (14). The coefficients on the edges are generated as

$$\Gamma_{ij} \sim \text{Unif}([0.2, 1]), \quad (i, j) \in E.$$

(M2) For the second model we let each bivariate distribution be given by the family of asymmetric Dirichlet distributions; see Example 3. We generate the two parameters of the bivariate Dirichlet models independently as

$$\alpha_1, \alpha_2 \sim \text{Unif}([1, 10]), \quad (i, j) \in E.$$

Note that the resulting d -dimensional Pareto distribution is not in the family of Dirichlet distributions.

We compare four different estimators for the weights on the minimum spanning tree $\hat{T}_\rho = (V, \hat{E}_\rho)$ in (16):

- (i) $\hat{\rho}_{ij} = -\log \hat{\chi}_{ij}$, where $\hat{\chi}_{ij}$ is the empirical extremal correlation;
- (ii) $\hat{\rho}_{ij} = \hat{\Gamma}_{ij}^{(m)}$, the extremal variogram estimator for one fixed $m \in V$;
- (iii) $\hat{\rho}_{ij} = \hat{\Gamma}_{ij}$, the combined extremal variogram estimator;
- (iv) $\hat{\rho}_{ij}$ are the censored negative log-likelihoods of the bivariate Hüsler–Reiss model (Y_i, Y_j) , evaluated at the optimizer.

The estimators (i)–(iii) were introduced in Section 4.2 and their consistency has been derived. The estimator in (iv) is the one used in Engelke and Hitz (2020) to learn the structure of Hüsler–Reiss tree models. Note that for this estimator, no theoretical justification is available. As performance measures we choose the average proportion of wrongly estimated edges

$$\mathbb{E}_{T=(V,E)} \mathbb{E} \left(1 - \frac{|\hat{E}_\rho \cap E|}{d-1} \right), \quad (18)$$

and the probability of not recovering the correct tree structure

$$\mathbb{E}_{T=(V,E)} \mathbb{P}(\hat{T}_\rho \neq T), \quad (19)$$

where the outer expectations signify that the tree T is randomly generated in each repetition. Each experiment is repeated 300 times in order to estimate these errors. We report only the results on the structure recovery rate error (19) and provide the corresponding results on the wrong edge rate (18) in the Supplementary Material S.1.

We first investigate the choice of the intermediate sequence $k = k_n$ of the number of exceedances used for estimation. We simulate from the Hüsler–Reiss tree model (M1) in dimension $d = 20$ and consider the minimum spanning trees \hat{T}_Γ and \hat{T}_{CL} based on the combined extremal variogram and the censored likelihoods, respectively. Figure 3 shows the structure recovery rate error as a function of the exceedance probability k/n for different samples sizes n . Interestingly, the two noise patterns lead to qualitatively different results: while consistent recovery of the limiting tree seems possible even when $k = n$ for noise model (N1), noise model (N2) with a dependence structure also introduces a bias in the corresponding minimal spanning tree and the true tree can not be recovered when the limit of k/n is too large. It is interesting to observe that the optimal exceedance probability k/n seems to converge to a positive value q^* , especially for noise (N1). This is consistent with the intuition given at the end of Section 4.2 in the paragraph after Remark 6. This is in contrast to classical asymptotic theory for consistent estimation in extremes where $k = o(n)$ is required to remove the approximation bias and therefore $q^* = 0$.

Next we compare the performance of the different structure learning methods for varying sample size n . Since the value of q^* which is required for consistent estimation is unknown in practice we choose $k = \lfloor n^{0.8} \rfloor$, which satisfies all assumptions of our theory. The results for dimension $d = 20$ are shown in the top row of Figure 4 for the Hüsler–Reiss model (M1) and in the bottom row for the asymmetric Dirichlet model (M2). We observe that the two methods based on the extremal variogram perform consistently better than the extremal correlation based method. Intuitively this can be explained by the fact that the extremal variogram is a tree metric for conditional independence of multivariate Pareto distributions. The additivity on the tree results in a bigger loss in the minimum spanning tree algorithm when choosing a wrong edge, and therefore it is easier to identify the true structure. The extremal correlation only satisfies a

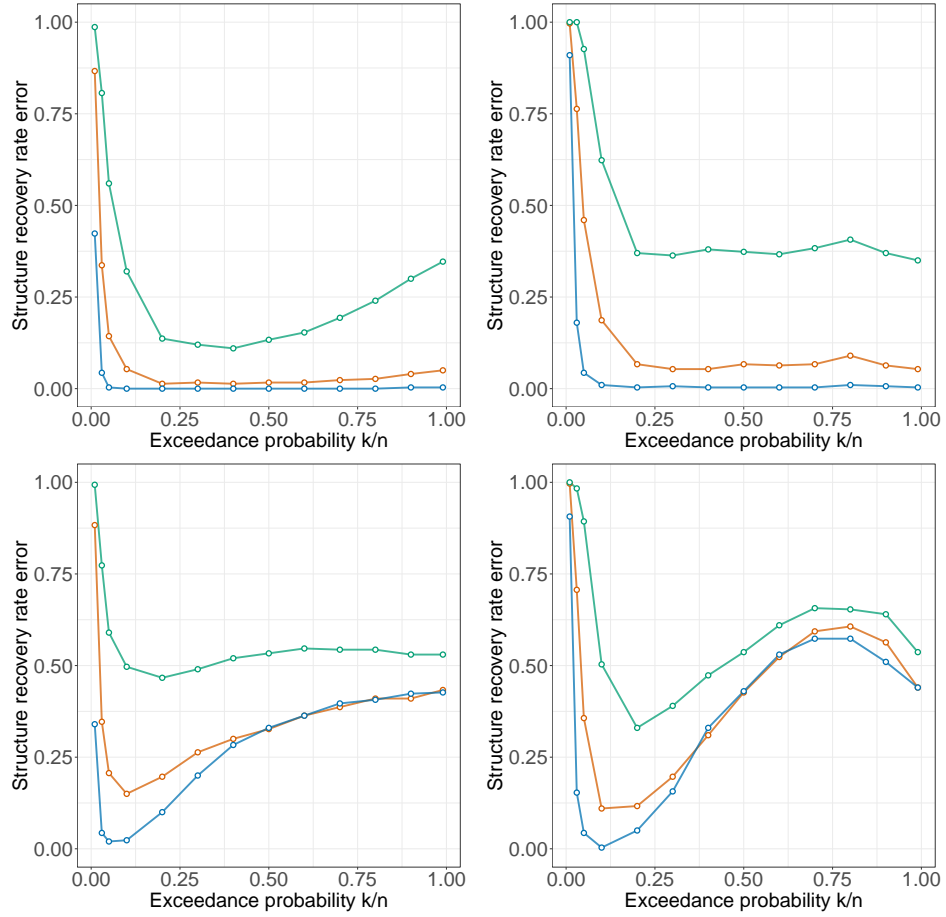


Figure 3: Structure recovery rate error of the combined empirical variogram estimator \hat{T}_Γ (left) and the censored likelihood estimator \hat{T}_{CL} (right) for the Hüsler–Reiss tree model (M1) and independent noise (N1) (top) and tree noise (N2) (bottom) in dimension $d = 20$ as a function of the exceedance probability k/n . Colors correspond to sample sizes $n = 500$ (green), $n = 1000$ (orange) and $n = 2000$ (blue).

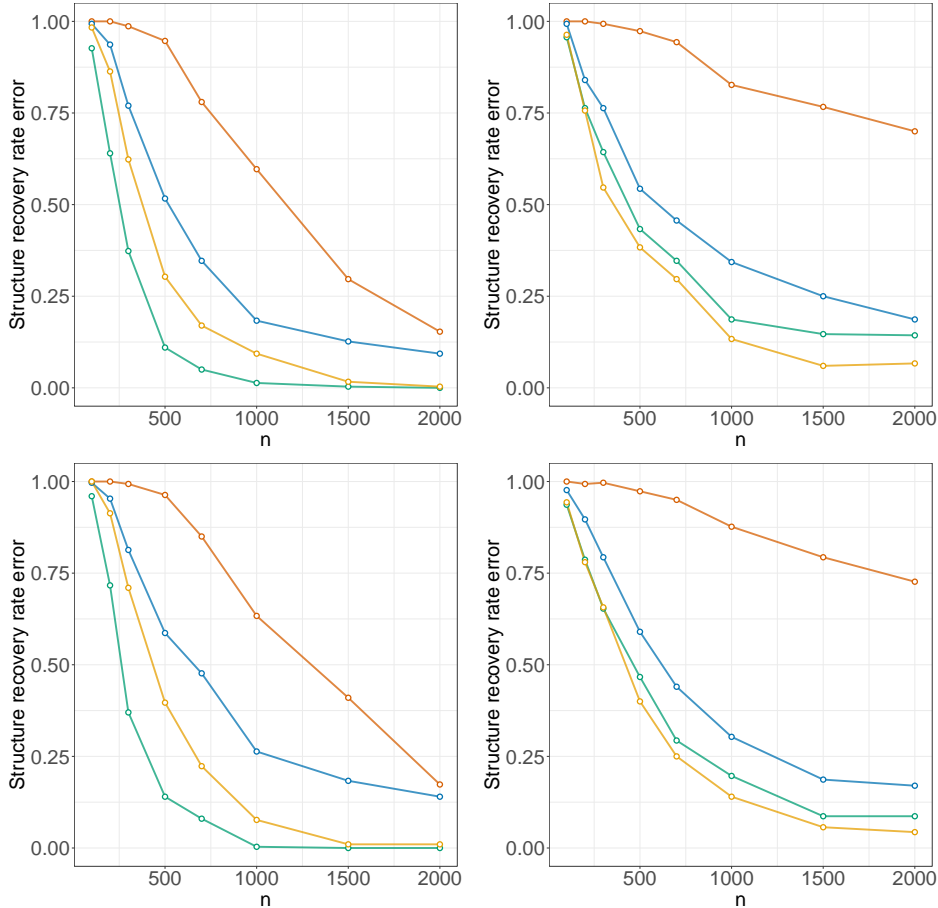


Figure 4: Structure recovery rate error of trees from the Hüsler–Reiss model (M1) (top) and Dirichlet model (M2) (bottom) in dimension $d = 20$ estimated based on empirical correlation (orange), extremal variogram with fixed $m \in V$ (blue), combined empirical variogram (green) and censored maximum likelihood (yellow); independent noise (N1) (left) and tree noise (N2) (right).

weaker relation (22) on the tree, which might be a reason for the higher error rate. Additionally, the empirical variogram uses information from the entire multivariate Pareto distribution, while the extremal correlation evaluates its distribution at a single point only. A comparison with the censored maximum likelihood estimator (iv) yields several insights. First, this approach seems to lead to consistent estimation of the tree structure even in model (M2) where \mathbf{Y} is not a Hüsler–Reiss distribution and the likelihood is thus misspecified. A possible explanation is that the strength of dependence is still sufficiently well estimated and the minimum spanning tree does only require correct ordering of the edge weights, which is much weaker than consistency of the estimated weights. Second, the different types of noise distributions in (N1) and (N2) lead to opposing orderings of the best method: whereas \hat{T}_{CL} has a slight advantage for noise (N2), \hat{T}_{Γ} performs substantially better under (N1). Notably, this is even the case in model (M1) where the likelihood is well-specified.

For the final set of comparisons we note that for a given tree, the task of estimating the correct structure can largely differ according to the strength of dependence of the multivariate Pareto distribution. We therefore conduct a simulation study where we fix $n = 500$ and $k = \lfloor n^{0.8} \rfloor$ and illustrate the performance of the structure estimation methods for a varying strength of tail dependence. For the Hüsler–Reiss model, we randomly generate a tree $T = (V, E)$ in dimension $d = 20$ and for $(i, j) \in E$ we fix all $\Gamma_{ij} = \lambda$ to some constant $\lambda > 0$. Equivalently, that

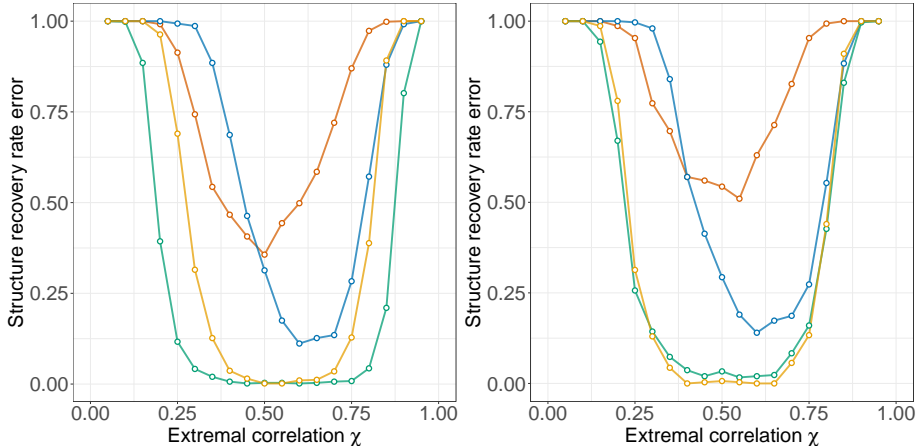


Figure 5: Structure recovery rate error for the Hüsler–Reiss model (M1) with noise model (N1) (left) and (N2) (right) in dimension $d = 20$ as a function of the extremal dependence between neighbors measured by the extremal correlation χ ; the different methods are based on empirical correlation (orange), extremal variogram with fixed $m \in V$ (blue), combined empirical variogram (green) and censored maximum likelihood (yellow).

means that all neighboring nodes have extremal correlation $\chi_{ij} = 2 - 2\Phi(\sqrt{\lambda}/2)$. The left panel of Figure 5 shows the results for varying strength of extremal dependence between neighbors measured by the extremal correlation under noise model (N1). Unsurprisingly the performance of all methods deteriorates at the boundaries, which correspond to the non-identifiable cases of independence and complete dependence. In general, it seems that the empirical variogram based estimators perform better under stronger dependence, which is probably due to the higher bias of the empirical extremal variogram under weak dependence. The same asymmetry can be observed for the censored maximum likelihood method, while the performance of the extremal correlation seems to be symmetric around $\chi = 1/2$. Comparing the performance of different methods, we observe that under noise (N1) the combined extremal variogram performs best uniformly in the values of χ , and the advantage over all other methods can be substantial. The same analysis with noise (N2) is shown in the right panel of Figure 5. In line with the results in Figure 4, the performance of \hat{T}_{CL} and \hat{T}_{Γ} is fairly similar, with a slight advantage for \hat{T}_{CL} at values of χ around 0.5 and the converse for χ closer to 0.2 and 0.8.

We close this section with some comments on computation times for the four estimators. The extremal correlation and variogram based trees rely on empirical estimators and are very efficient to compute. The censored likelihood estimator however requires numerical optimization for every weight ρ_{ij} , $i, j \in V$. Especially in higher dimensions this becomes prohibitively costly. Figure 12 in the Supplementary Material S.3 shows the average computation times for the four estimators in the simulations in Figure 4. It can be seen that the censored likelihood method is several orders of magnitude slower than the empirical methods.

6 Application

We illustrate the proposed methodology on foreign exchange rates of $d = 26$ currencies expressed in terms of the British Pound sterling; see Table 1 in Appendix A for the three-letter abbreviations of the respective countries. The data are available from the website of the Bank of England¹. They consist of daily observations of spot foreign exchange rates in the period from 1 October 2005 to 30 September 2020, resulting in $n = 3790$ observations.

¹<https://www.bankofengland.co.uk/>

In order to obtain time series without temporal dependence, we pre-process the data set. We first compute the daily log-returns R_{ij} , $i = 1, \dots, n$, $j = 1, \dots, d$, from the original time series. To remove the serial dependence, we then filter the univariate series by ARMA-GARCH processes; see Hilal et al. (2014) for a similar approach, and Bollerslev et al. (1992) and Engle (1982) for background on financial time series modeling. The AIC suggest that an ARMA(0, 2)-GARCH(1, 1) model is the most appropriate for most of the univariate series. We derive the absolute values of the standardized filtered returns as

$$X_{ij} = \left| \frac{R_{ij} - \hat{\mu}_{ij}}{\hat{\sigma}_{ij}} \right|,$$

where $\hat{\mu}_{ij}$ and $\hat{\sigma}_{ij}$ are the estimated mean and standard deviation of the ARMA-GARCH model. The absolute value means that we are interested in extremes in both directions.

The data $\mathbf{X}_i = (X_{i1}, \dots, X_{id})$ are approximately independent and identically distributed for $i = 1, \dots, n$, and we will model their tail dependence using an extremal tree model. We first check whether the assumption of asymptotic dependence is satisfied by inspecting the behavior of the function $q \mapsto \hat{\chi}_{ij}(q)$ for values $q = k/n$ close to 1. For most of the pairs this function seems to converge to a positive value and thus there is fairly strongly dependence in the tail between the filtered log-returns; see Figure 11 in the Supplementary Material 11 for some examples.

Motivated by the simulations in the previous section we estimate the extremal tree structure $\hat{T}_\Gamma = (V, \hat{E}_\Gamma)$ non-parametrically using the combined empirical extremal variogram $\hat{\Gamma}$. The corresponding minimum spanning tree for a threshold of $q = 0.05$ is shown in Figure 6; we note that the tree is very stable across different values of q close to 0. The structure of the tree allows for a nice interpretation of extremal dependence. Extreme observations in the exchange rates with the Euro are strongly connected with extremes of other European currencies in Northern and Eastern countries. The graph suggests that extremes of exchange rates of these currencies are conditionally independent of exchange rates of other countries, given the value of Euro exchange rate. The Malaysian ringgit, the Chinese yuan, the Hong Kong dollar and the Taiwan dollar are strongly pegged to the US dollar and their closeness in the tree is therefore not surprising. Another branch of the tree contains several currencies of the Commonwealth. Finally, the connection between Japan and Switzerland is plausible because both currencies can be considered safe-haven currencies, which are both popular investments in times of crises.

In order to address the stability of the tree structure we bootstrap our data $B = 100$ times and fit each time the tree structure. Figure 7 shows that graph where the width of each edge is proportional to the number of times it has been selected in an extremal tree. Overall, the tree seems to be fairly stable since there is only a small number of dominant edges. Moreover, we can identify clear clusters that are connected in most of the trees, such as the European currencies. On the other hand some currencies such as the Russian ruble that do not have a dominant connection to any of these clusters. In future research, it could therefore be interesting to study structure estimation for forests, which allow to have unconnected graphs whose connected components are trees (Liu et al., 2011).

So far we have not assumed any specific model for the extremal dependence on the edges since we are able to estimate the tree structure fully non-parametrically with the methods from this paper. If we were only interested in interpretation of the extremal graphical structure we could stop our analysis here. If we require a model for rare event simulation or risk assessment, in a second step we can choose arbitrary bivariate Pareto models for each edge. For simplicity, we choose here for all edges the Hüsler–Reiss model (see Example 4) resulting in a Hüsler–Reiss tree. For this model, the bivariate parameter estimates $\hat{\Gamma}_{ij}$ can be chosen directly as the empirical extremal variogram estimates for all $\{i, j\} \in \hat{E}_\Gamma$. Alternatively, we could estimate them by censored maximum likelihood. In both cases, the remaining entries of the Hüsler–Reiss parameter matrix can be obtained from the additivity of the extremal variogram on the tree in (14). Figure 8 shows the extremal correlations implied by the fitted Hüsler–Reiss tree model

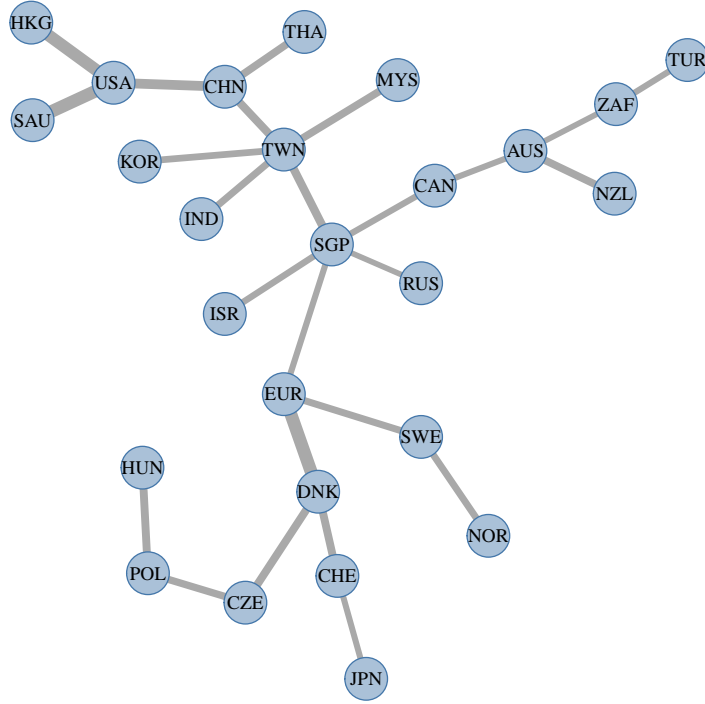


Figure 6: Minimum spanning tree \hat{T}_Γ of extremal dependence for the spot foreign exchange rate data based on the combined extremal variogram. The width of each edge $(i, j) \in \hat{E}_\Gamma$ is proportional to the extremal correlation $2 - 2\Phi(\sqrt{\hat{\Gamma}_{ij}}/2)$, and therefore wider edges indicate stronger extremal dependence.

against the empirical counterparts $\hat{\chi}_{ij}$, $i, j \in V$. Even though the tree structure is a very sparse graph with only $d - 1$ edges, the extremal dependence between all variables is well-explained.

Acknowledgments

The authors would like to thank Jiaying Gu for pointing us to Hall's marriage theorem, and Nicola Gnecco, Adrien S. Hitz, Michaël Lalancette and Chen Zhou for helpful comments. Sebastian Engelke was supported by an Eccellenza grant of the Swiss National Science Foundation and Stanislav Volgushev was partially supported by a discovery grant from NSERC of Canada.

Appendix

A Country codes used in the application in Section 6

Table 1 shows the three-letter country codes of the exchange rates into British Pound sterling.

B Proof of Proposition 2

The assertions of (i) and (ii) follow immediately from the definition of \mathbf{W}^m in (4) and the fact that $\Gamma^{(m)}$ is the variogram matrix of this random vector.

For (iii), the convergence $\chi_{im}(n) \rightarrow 0$ implies that the corresponding extremal functions $W_i^m(n)$ converge to 0 almost surely. Indeed, we have for any $x \in (0, 1)$

$$\chi_{im}(n) = \mathbb{P}(Y_i^m(n) > 1) = \mathbb{P}(PW_i^m(n) > 1) \geq x\mathbb{P}(PW_i^m(n) > 1 \mid P > 1/x) = x\mathbb{P}(W_i^m(n) > x),$$

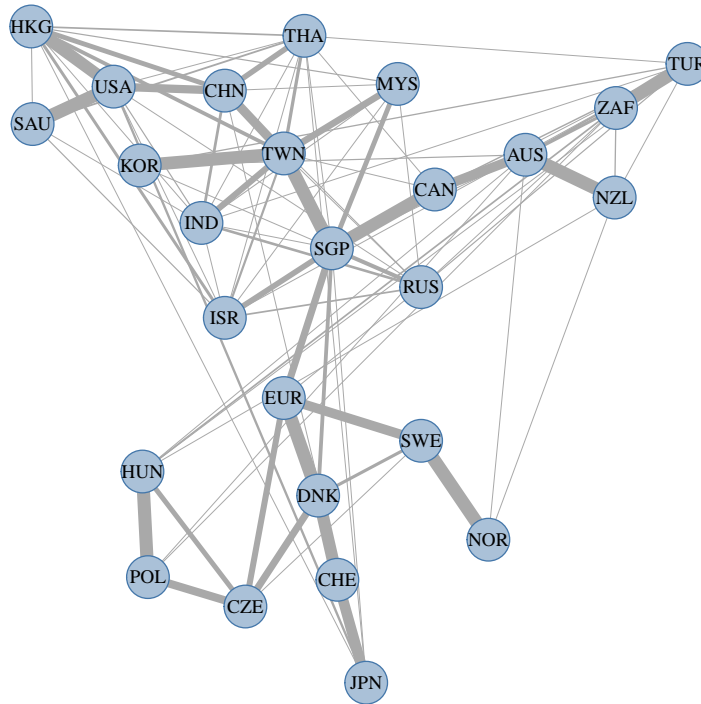


Figure 7: Graph where the width of each edge is proportional to the number of times it has been selected in an extremal tree in the bootstrap procedure.

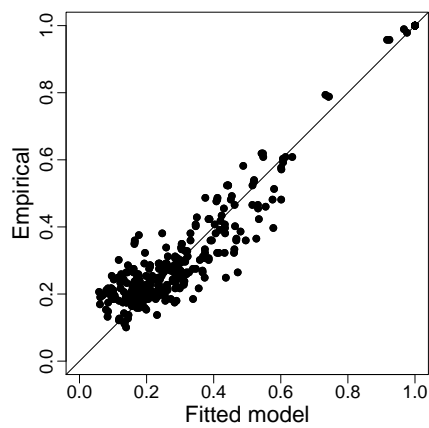


Figure 8: Extremal correlations for the spot foreign exchange rate data implied by the fitted Hüsler–Reiss tree model against the empirical counterparts.

Table 1: Three-letter country codes.

Code	Foreign Exchange Rate (into GBP)	Code	Foreign Exchange Rate (into GBP)
AUS	Australian Dollar	NOR	Norwegian Krone
CAN	Canadian Dollar	POL	Polish Zloty
CHN	Chinese Yuan	RUS	Russian Ruble
CZE	Czech Koruna	SAU	Saudi Riyal
DNK	Danish Krone	SGP	Singapore Dollar
EUR	Euro	ZAF	South African Rand
HKG	Hong Kong Dollar	KOR	South Korean Won
HUN	Hungarian	SWE	Swedish Krona
IND	Indian Rupee	CHE	Swiss Franc
ISR	Israeli Shekel	TWN	Taiwan Dollar
JPN	Japanese Yen	THA	Thai Baht
MYS	Malaysian ringgit	TUR	Turkish Lira
NZL	New Zealand Dollar	USA	US Dollar

which shows that $\mathbb{P}(W_i^m(n) > x) \rightarrow 0$ as $n \rightarrow \infty$. This yields that $\Gamma_{im}^{(m)}(n) \rightarrow \infty$ as $n \rightarrow \infty$. \square

C Proof of Proposition 4

In order to show that the extremal variogram $\Gamma^{(m)}$ defines a tree metric on T , we recall the stochastic representation of \mathbf{Y}^m in Proposition 1. We compute

$$\Gamma_{ij}^{(m)} = \text{Var} \left\{ \sum_{e \in \text{ph}(mi)} \log W_e - \sum_{\tilde{e} \in \text{ph}(mj)} \log W_{\tilde{e}} \right\} = \sum_{e \in \text{ph}(ij)} \text{Var} \{ \log W_e \} = \sum_{(s,t) \in \text{ph}(ij)} \Gamma_{st}^{(m)},$$

where the second to last equality follows from the independence of the $\{W_e : e \in E\}$. Moreover, for the last equation we note that for two neighboring nodes $(s, t) \in E^m$ in the directed tree T^m , by applying the same argument as above, we have $\Gamma_{st}^{(s)} = \text{Var} \{ \log W_t^s \} = \Gamma_{st}^{(m)}$. \square

D Proof of Corollary 1

We have to show that for any tree $T' = (V, E')$ that differs from T in at least one edge, it holds

$$\sum_{(i,j) \in E'} \Gamma_{ij}^{(m)} - \sum_{(i,j) \in E} \Gamma_{ij}^{(m)} > 0. \quad (20)$$

The terms for $(i, j) \in E \cap E'$ cancel directly between the two sums. For $(i, j) \in E \setminus E'$, the graph $(V, E \setminus \{(i, j)\})$ is disconnected with connected components, say, $V_1, V_2 \subset V$. Since T' is connected, there must be a $h \in V_1$ and $l \in V_2$ such that $(h, l) \in E'$. Since the path $\text{ph}(hl)$ on the tree T must contain the edge (i, j) and

$$\Gamma_{hl}^{(m)} = \sum_{e \in \text{ph}(hl)} \Gamma_e^{(m)}, \quad (21)$$

this means that the first sum in (23) contains $\Gamma_{ij}^{(m)}$ as part of $\Gamma_{hl}^{(m)}$, which cancels the corresponding term in the second sum.

There are the same number of edges in $E \setminus E'$ as in $E' \setminus E$ and every $\Gamma_{hl}^{(m)}$ for $(h, l) \in E \setminus E'$ is the sum of several terms in the decomposition 26. Therefore, the difference on the left-hand side of (23) is indeed strictly positive as long as none of the distances vanishes. \square

E Proof of Corollary 2

For the true edge set E we observe

$$\begin{aligned} \sum_{(i,j) \in E} \rho_{ij} &= \sum_{(i,j) \in E} \sum_{m=1}^d w_m \Gamma_{ij}^{(m)} < \sum_{m=1}^d w_m \min_{T \neq T' = (V, E')} \sum_{(i,j) \in E'} \Gamma_{ij}^{(m)} \\ &\leq \min_{T \neq T' = (V, E')} \sum_{(i,j) \in E'} \sum_{m=1}^d w_m \Gamma_{ij}^{(m)} = \min_{T \neq T' = (V, E')} \sum_{(i,j) \in E'} \rho_{ij}, \end{aligned}$$

where the first inequality follows from the uniqueness of the minimum spanning tree with weights $\Gamma_{ij}^{(m)}$, $m \in V$. It follows that $T = (V, E)$ must be the minimum spanning tree corresponding to the weights $\rho_{ij} = \sum_{m=1}^d w_m \Gamma_{ij}^{(m)}$. \square

F Proof of Proposition 5

First note that $\chi_{ij} > 0$ for all $i, j \in V$ since the tree is connected and there cannot be two independent components of \mathbf{Y} . While the extremal correlation coefficients do not form a tree metric, they still satisfy a weaker relation on the tree T , namely

$$\chi_{hl} \leq \chi_{ij} \quad \forall (i, j) \in \text{ph}(hl), \quad (22)$$

and the inequality is strict as soon as $(i, j) \neq (h, l)$. To prove this, we note that we can write the extremal correlation χ_{hl} in the extremal tree model \mathbf{Y} as

$$\chi_{hl} = \mathbb{P}(Y_l > 1 \mid Y_h > 1) = \mathbb{P}(Y_l^h > 1).$$

From (8) we have that

$$Y_l^h = P \prod_{e \in \text{ph}(hl)} W_e,$$

and therefore, by independence between P and $\{W_e : e \in \text{ph}(hl)\}$ and since P follows a standard Pareto distribution,

$$\chi_{hl} = \int_1^\infty u^{-2} \mathbb{P}\left(u > \prod_{e \in \text{ph}(hl)} 1/W_e\right) dx = \mathbb{E}\left[\min\left(\prod_{e \in \text{ph}(hl)} W_e, 1\right)\right],$$

by changing the order of integration. Observe that for any two positive, independent random variables A and B with $\mathbb{E}A, \mathbb{E}B \leq 1$, we have from Jensen's inequality by concavity of $x \mapsto \min(x, 1)$

$$\mathbb{E}[\min(AB, 1)] = \mathbb{E}\{\mathbb{E}[\min(AB, 1) \mid A]\} \leq \mathbb{E}\{\min[A\mathbb{E}(B \mid A), 1]\} = \mathbb{E}[\min(A, 1)],$$

with equality if and only if $B = 1$ almost surely. Since the distribution \mathbf{Y} is non-degenerate, there is no W_e , $e \in E$, with $W_e = 1$ almost surely, and moreover $\mathbb{E}W_e \leq 1$. Since $(i, j) \in \text{ph}(hl)$ we can apply the above successively to obtain

$$\chi_{hl} = \mathbb{E}\left[\min\left(\prod_{e \in \text{ph}(hl)} W_e, 1\right)\right] \leq \mathbb{E}[\min(W_{(i,j)}, 1)] = \chi_{ij}.$$

Thus (22) follows. We now continue with the main proof. We have to show that for any tree $T' = (V, E')$ that differs from T in at least one edge, it holds

$$\sum_{(i,j) \in E'} \rho_{ij} - \sum_{(i,j) \in E} \rho_{ij} > 0, \quad (23)$$

where we let $\rho_{ij} = -\log(\chi_{ij}) > 0$.

We will now compare the summands in the two sums in (23) in a pairwise fashion. To this end, we will construct a bijective mapping $\tau : E \rightarrow E'$ such that for any $(i, j) \in E$, the corresponding edge $(h, l) = \tau\{(i, j)\} \in E'$ satisfies $(i, j) \in \text{ph}(hl; T)$, where for clarity we indicate that the path in the tree T is meant.

To this end consider the graph undirected $G = (E + E', \mathcal{E})$ where $(i, j) \in E$ is connected to $(h, l) \in E'$ if and only if $(i, j) \in \text{ph}(hl; T)$. In this formulation, our goal is to find an E -saturating matching, that is, a matching such that every element of E is assigned one element in E' . A graphical illustration of this idea is provided in Figure 9.

By Hall's marriage theorem (Hall, 1935), such a matching exists provided that for any subset $C \subset E$, the corresponding neighborhood $n(C) \subset E'$ of elements in E' that are connected to at least one of the elements in C satisfies

$$|C| \leq |n(C)|. \quad (24)$$

Let e_1, \dots, e_p be the edges in C , where $p = |C|$. Removing these edges from the tree $T = (V, E)$ results in a graph $(V, E \setminus C)$ with $p+1$ connected components, which we denote by V_1, \dots, V_{p+1} .

Starting with component V_1 , we know from the connectedness of the tree T' that there must be an edge in E' between at least one of the elements of V_1 , say h_1 , to $l_1 \in V_{k_1}$ for some $k_1 \neq 1$. Since h_1 and l_1 are in different connected components in $(V, E \setminus C)$, the path $\text{ph}(h_1 l_1; T)$ must contain one of the edges in C , and therefore $e'_1 = (h_1, l_1) \in n(C)$.

Similarly, there must exist an edge $e'_2 = (h_2, l_2)$ between an element $h_2 \in V_1 \cup V_{k_1}$ and some $l_2 \in V_{k_2}$, $k_2 \notin \{1, k_1\}$. This edge is necessarily different from e'_1 as it has a node in V_{k_2} , and the path $\text{ph}(h_2 l_2; T)$ must contain one of the edges in C because h_2, l_2 are in different connected components of $(V, E \setminus C)$. Thus $e'_2 \in n(C)$.

Continuing this argument inductively we obtain p different edges in $n(C)$ and therefore the condition (24) holds.

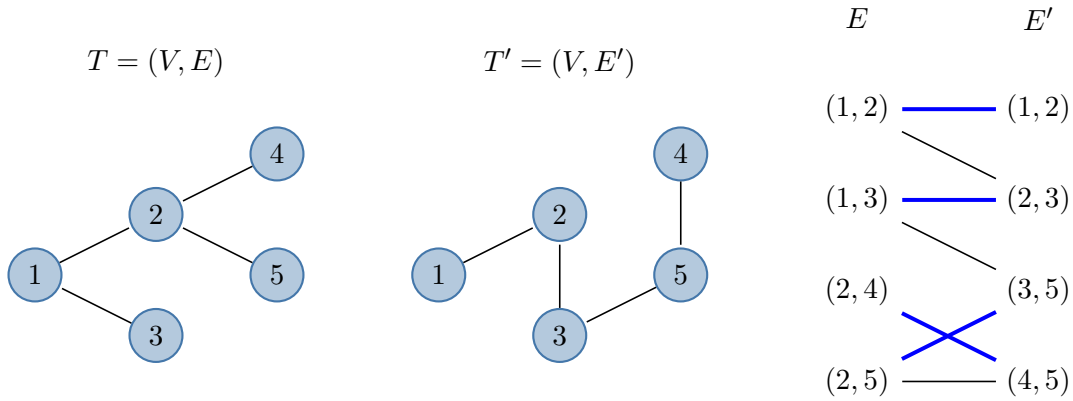


Figure 9: Left and center: two trees T and T' . Right: bipartite graph between elements in E and E' . A link from $(i, j) \in E$ to $(h, l) \in E'$ means that $(i, j) \in \text{ph}(hl; T)$. The blue links indicate one possible matching $\tau : E \rightarrow E'$ in this case.

In order to show inequality (23) we rewrite the left-hand side as

$$\sum_{(i,j) \in E} (\rho_{\tau\{(i,j)\}} - \rho_{ij}). \quad (25)$$

By construction of τ , for $(h, l) = \tau\{(i, j)\}$, the path $\text{ph}(hl)$ on the tree T must contain the edge (i, j) and thus by (22)

$$\rho_{hl} \geq \max_{e \in \text{ph}(hl)} \rho_e \geq \rho_{ij}. \quad (26)$$

This means that all summands in (25) are non-negative. Since there is at least one $(h, l) \in E' \setminus E$, the first inequality in (26) is strict for this edge and therefore, the difference on the left-hand side of (23) is indeed strictly positive. Thus the proof is complete. \square

References

- Asenova, S., G. Mazo, and J. Segers (2020). Inference on extremal dependence in a latent markov tree model attracted to a Hüsler–Reiss distribution. Available from <https://arxiv.org/abs/2001.09510>.
- Bollerslev, T., R. Y. Chou, and K. F. Kroner (1992). Arch modeling in finance: A review of the theory and empirical evidence. *Journal of Econometrics* 52(1), 5 – 59.
- Chilès, J.-P. and P. Delfiner (2012). *Geostatistics* (Second ed.). Wiley Series in Probability and Statistics. John Wiley & Sons, Inc., Hoboken, NJ. Modeling spatial uncertainty.
- Chow, C. and C. Liu (1968). Approximating discrete probability distributions with dependence trees. *IEEE Transactions on Information Theory* 14, 462–467.
- Coles, S., J. Heffernan, and J. Tawn (1999). Dependence measures for extreme value analyses. *Extremes* 2, 339–365.
- Coles, S. G. and J. A. Tawn (1991). Modelling extreme multivariate events. *Journal of the Royal Statistical Society. Series B. Methodological* 53(2), 377–392.
- Cooley, D., P. Naveau, and P. Poncet (2006). Variograms for spatial max-stable random fields. In P. Bertail, P. Soulier, and P. Doukhan (Eds.), *Dependence in Probability and Statistics*, Volume 187 of *Lecture Notes in Statistics*, Chapter 17, pp. 373–390. New York: Springer.
- Cooley, D. and E. Thibaud (2019). Decompositions of dependence for high-dimensional extremes. *Biometrika* 106(3), 587–604.
- Cowell, R. G., P. Dawid, S. L. Lauritzen, and D. J. Spiegelhalter (2006). *Probabilistic networks and expert systems: Exact computational methods for Bayesian networks*. Springer.
- Csörgő, M. and L. Horváth (1987). Approximation of intermediate quantile processes. *Journal of Multivariate Analysis* 21(2), 250–262.
- Dawid, A. P. (1979). Conditional independence in statistical theory. *Journal of the Royal Statistical Society. Series B (Methodological)* 41, 1–31.
- Dombry, C., S. Engelke, and M. Oesting (2016). Exact simulation of max-stable processes. *Biometrika* 103, 303–317.
- Dombry, C. and F. Éyi-Minko (2013). Regular conditional distributions of continuous max-infinitely divisible random fields. *Electron. J. Probab.* 18.
- Drton, M. t. and M. H. Maathuis (2017). Structure learning in graphical modeling. *Annual Review of Statistics and Its Application* 4(1), 365–393.
- Einmahl, J. H., A. Krajina, J. Segers, et al. (2012). An m-estimator for tail dependence in arbitrary dimensions. *The Annals of Statistics* 40(3), 1764–1793.
- Einmahl, J. H. J., A. Kiriliouk, A. Krajina, and J. Segers (2016). An M-estimator of spatial tail dependence. *J. R. Stat. Soc. Ser. B Stat. Methodol.* 78, 275–298.

- Engelke, S., R. de Fondeville, and M. Oesting (2019). Extremal behaviour of aggregated data with an application to downscaling. *Biometrika* 106, 127–144.
- Engelke, S. and A. Hitz (2020). Graphical models for extremes (with discussion). *J. R. Stat. Soc. Ser. B Stat. Methodol.* 82, 871–932.
- Engelke, S., S. A. Hitz, and N. Gnecco (2019). *graphicalExtremes: Statistical Methodology for Graphical Extreme Value Models*. Available from <https://CRAN.R-project.org/package=graphicalExtremes>, R package version 0.1.0.
- Engelke, S. and J. Ivanovs (2021). Sparse structures for multivariate extremes. *Annual Review of Statistics and Its Application* 8. To appear.
- Engelke, S., A. Malinowski, Z. Kabluchko, and M. Schlather (2015). Estimation of Hüsler–Reiss distributions and Brown–Resnick processes. *Journal of the Royal Statistical Society. Series B. Methodological* 77(1), 239–265.
- Engle, R. F. (1982). Autoregressive conditional heteroscedasticity with estimates of the variance of united kingdom inflation. *Econometrica* 50(4), 987–1007.
- Fomichov, V. and J. Ivanovs (2020). Detection of groups of concomitant extremes using clustering. Available from <https://arxiv.org/abs/2010.12372>.
- Fougères, A.-L., L. De Haan, C. Mercadier, et al. (2015). Bias correction in multivariate extremes. *The Annals of Statistics* 43(2), 903–934.
- Gissibl, N. and C. Klüppelberg (2018). Max-linear models on directed acyclic graphs. *Bernoulli* 24, 2693–2720.
- Hall, P. (1935). On representatives of subsets. *J. London Math. Soc.* 10, 26–30.
- Hilal, S., S.-H. Poon, and J. Tawn (2014). Portfolio risk assessment using multivariate extreme value methods. *Extremes* 17, 531–556.
- Kabluchko, Z., M. Schlather, and L. de Haan (2009). Stationary max-stable fields associated to negative definite functions. *Ann. Probab.* 37, 2042–2065.
- Katz, R. W., M. B. Parlange, and P. Naveau (2002). Statistics of extremes in hydrology. *Advances in Water Resources* 25, 1287–1304.
- Klüppelberg, C. and S. Lauritzen (2019). *Bayesian Networks for Max-Linear Models*, pp. 79–97. Cham: Springer International Publishing.
- Kruskal, Jr., J. B. (1956). On the shortest spanning subtree of a graph and the traveling salesman problem. *Proceedings of the American Mathematical Society* 7, 48–50.
- Lafferty, J., H. Liu, and L. Wasserman (2012). Sparse nonparametric graphical models. *Statist. Sci.* 27, 519–537.
- Larsson, M. and S. I. Resnick (2012). Extremal dependence measure and extremogram: the regularly varying case. *Extremes* 15, 231–256.
- Lauritzen, S. L. (1996). *Graphical Models*. Oxford University Press.
- Liu, H., M. Xu, H. Gu, A. Gupta, J. Lafferty, and L. Wasserman (2011). Forest density estimation. *The Journal of Machine Learning Research* 12, 907–951.
- Papastathopoulos, I. and K. Strokorb (2016). Conditional independence among max-stable laws. *Statistics & Probability Letters* 108, 9–15.

- Poon, S.-H., M. Rockinger, and J. Tawn (2004). Extreme value dependence in financial markets: Diagnostics, models, and financial implications. *Rev. Financ. Stud.* 17, 581–610.
- Prim, R. C. (1957). Shortest connection networks and some generalizations. *Bell System Technical Journal* 36, 1389–1401.
- Radulović, D., M. Wegkamp, and Y. Zhao (2017). Weak convergence of empirical copula processes indexed by functions. *Bernoulli* 23(4B), 3346–3384.
- Resnick, S. I. (2008). *Extreme Values, Regular Variation and Point Processes*. New York: Springer.
- Rootzén, H., J. Segers, and J. L. Wadsworth (2018). Multivariate peaks over thresholds models. *Extremes* 21(1), 115–145.
- Rootzén, H. and N. Tajvidi (2006). Multivariate generalized Pareto distributions. *Bernoulli* 12, 917–930.
- Schlather, M. and J. A. Tawn (2003). A dependence measure for multivariate and spatial extreme values: properties and inference. *Biometrika* 90, 139–156.
- Segers, J. (2019). One- versus multi-component regular variation and extremes of Markov trees. Available from <https://arxiv.org/abs/1902.02226>.
- Wackernagel, H. (2013). *Multivariate geostatistics*. Springer, New York. an introduction with applications.

Supplementary Material

S.1 Additional simulation results

Figure 10 shows the wrong edge rate (18) for the simulation study in Figure 4.

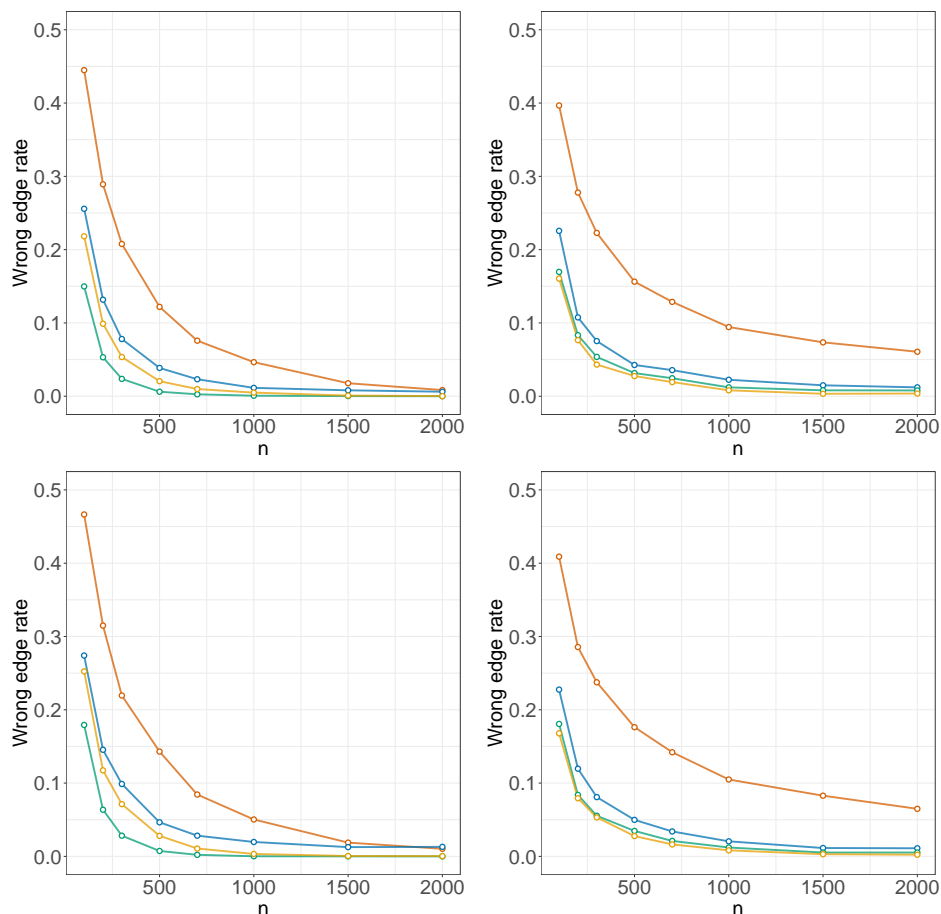


Figure 10: Wrong edge rate of trees from the Hüsler–Reiss model (M1) (top) and Dirichlet model (M2) (bottom) in dimension $d = 20$ estimated by the different methods based on empirical correlation (orange), extremal variogram with fixed $m \in V$ (blue), combined empirical variogram (green) and censored maximum likelihood (yellow); independent noise model (N1) (left) and tree noise model (N2) (right).

S.2 Plots of $\hat{\chi}$ the application in Section 6

Figure 11 shows plots of the estimated $\hat{\chi}_{ij}(q)$ coefficient for different pairs of exchange rates.

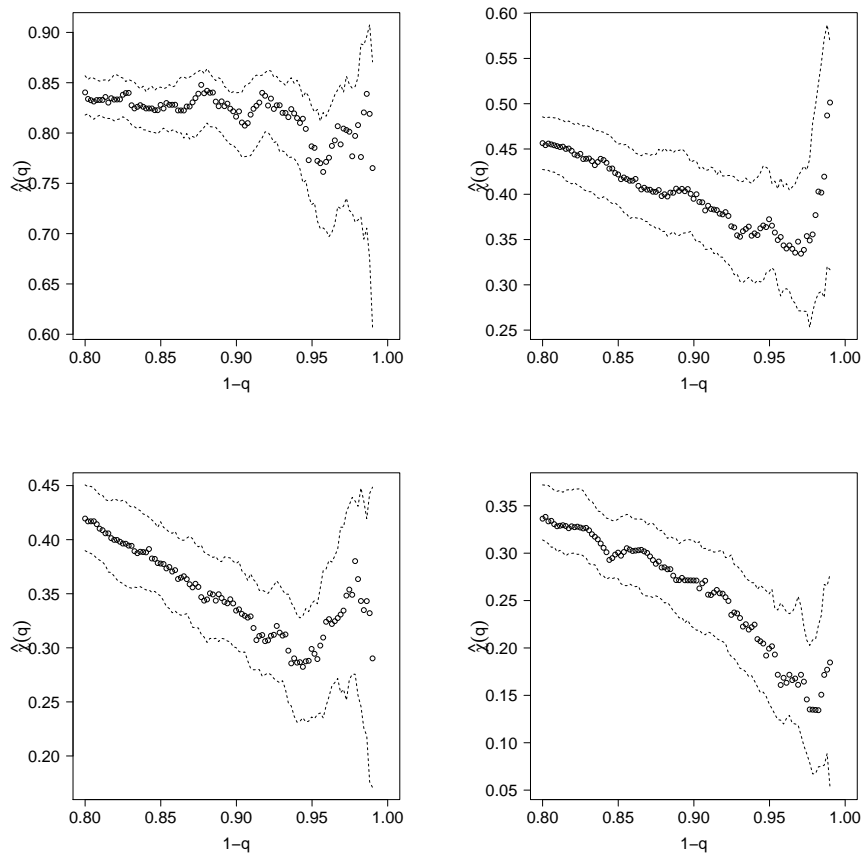


Figure 11: Plots of the function $q \mapsto \hat{\chi}_{ij}(q)$ for values $q = k/n$ between 0.8 and 1 for four different pairs of exchange rates (all in terms of British Pound sterling); from left to right and top to bottom: CHN/USA, EUR/SGP, CAN/HKG, POL/RUS.

S.3 Computation time of algorithms

Figure 12 shows the computation times of the different tree estimation methods.

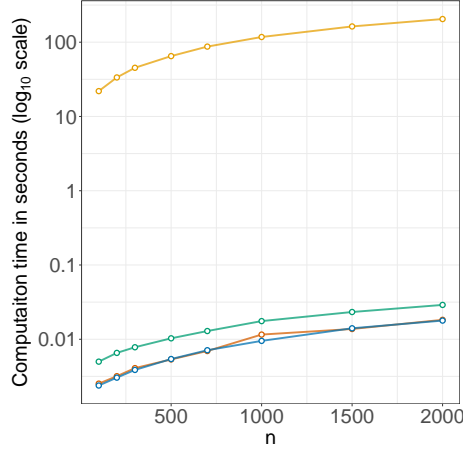


Figure 12: Average computation times in seconds (on base-10 logarithm scale) in the simulation studies in Section 5 of the four algorithms based on empirical correlation (orange), extremal variogram with fixed $m \in V$ (blue), combined empirical variogram (green) and censored maximum likelihood (yellow).

S.4 Proof of Proposition 1

Without loss of generality, let $m = 1$ and suppose that d is a terminal node of the directed tree T^m and node $d - 1$ is its only parent; this can always be achieved by renaming nodes. It follows from the global Markov property that

$$Y_d^{d-1} \perp\!\!\!\perp \mathbf{Y}_{\setminus\{d-1,d\}}^{d-1} \mid \mathbf{Y}_{d-1}^{d-1}.$$

Recalling the representation $\mathbf{Y}^{d-1} = P\mathbf{W}^{d-1}$ from (4), we can rewrite this to

$$PW_d^{d-1} \perp\!\!\!\perp PW_{\setminus d}^{d-1} \mid P,$$

where P is a standard Pareto random variable which is independent of W^{d-1} and since $W_{d-1}^{d-1} = 1$ almost surely. This implies that $W_d^{d-1} \perp\!\!\!\perp \mathbf{W}_{\setminus\{d-1,d\}}^{d-1}$ are unconditionally independent. In the sequel, we use an identity that relates the distributions of extremal functions with respect to the different components $m = 1$ and $d - 1$. For any continuous, bounded function $h : [1, \infty) \times [0, \infty)^{d-1} \rightarrow [0, \infty)$ we have

$$\mathbb{E}[\mathbf{1}\{W_{d-1}^m > 0\}h(\mathbf{W}^m)] = \mathbb{E}\left[h(\mathbf{W}^{d-1}/W_m^{d-1})W_m^{d-1}\right]; \quad (27)$$

see for instance Segers (2019, Cor. 3), or similar representations in Dombry and Éyi-Minko (2013, Prop. 4.2) and Dombry et al. (2016, Prop. 1).

We first consider the distribution of \mathbf{Y}^m on the set $\{Y_{d-1}^m > 0\}$. Observe that for any continuous, bounded function $f : [1, \infty) \times [0, \infty)^{d-1} \rightarrow [0, \infty)$ and any $u > 0$ we have

$$\mathbb{E}[f(u\mathbf{W}^{d-1}/W_m^{d-1})W_m^{d-1}] = \mathbb{E}[\mathbb{E}\{f(u\mathbf{W}^{d-1}/W_m^{d-1})W_m^{d-1} \mid W_d^{d-1}\}] = \mathbb{E}[g(u, W_d^{d-1})]$$

where, noting that $W_{d-1}^{d-1} = 1$ almost surely

$$\begin{aligned} g(u, v) &:= \mathbb{E}[f(u\mathbf{W}_{\setminus d}^{d-1}/W_m^{d-1}, uvW_{d-1}^{d-1}/W_m^{d-1})W_m^{d-1}] \\ &= \mathbb{E}[f(u\mathbf{W}_{\setminus d}^m, uvW_{d-1}^m)\mathbf{1}\{W_{d-1}^m > 0\}] \end{aligned}$$

Here, the second equality in the representation for g follows by (27) applied with

$$h(w_1, \dots, w_d) := f(uw_1, \dots, uw_{d-1}, uvw_{d-1}).$$

Thus we obtain for bounded, continuous functions $f : [1, \infty) \times [0, \infty)^{d-1} \rightarrow [0, \infty)$

$$\begin{aligned} & \mathbb{E} [\mathbf{1}\{Y_{d-1}^m > 0\} f(\mathbf{Y}^m)] = \mathbb{E} [\mathbf{1}\{W_{d-1}^m > 0\} f(P\mathbf{W}^m)] \\ &= \int_1^\infty u^{-2} \mathbb{E} [\mathbf{1}\{W_{d-1}^m > 0\} f(u\mathbf{W}^m)] du \\ &\stackrel{\text{by (27)}}{=} \int_1^\infty u^{-2} \mathbb{E} [f(u\mathbf{W}^{d-1}/W_m^{d-1})W_m^{d-1}] du \\ &\stackrel{(a)}{=} \int_1^\infty u^{-2} \int_{[0, \infty)} \mathbb{E} [\mathbf{1}\{W_{d-1}^m > 0\} f(u\mathbf{W}_{\setminus d}^m, uW_{d-1}^m w_d)] \mathbb{P}(W_d^{d-1} = dw_d) du \\ &= \mathbb{E} [\mathbf{1}\{Y_{d-1}^m > 0\} f(\mathbf{Y}_{\setminus d}^m, Y_{d-1}^m \tilde{W}_d^{d-1})] \end{aligned} \quad (28)$$

where \tilde{W}_d^{d-1} is an independent copy of W_d^{d-1} , also independent of all the other random variables in the above equation, and equation (a) uses the representation for $\mathbb{E}[f(u\mathbf{W}^{d-1}/W_m^{d-1})W_m^{d-1}]$ derived earlier.

If $\mathbb{P}(Y_{d-1}^m = 0) > 0$, it remains to consider the term $\mathbb{E} [\mathbf{1}\{Y_{d-1}^m = 0\} f(\mathbf{Y}^m)]$. From $Y_d^m \perp\!\!\!\perp \mathbf{Y}_{\setminus \{d-1, d\}}^m \mid Y_{d-1}^m$ it follows for any $s \geq 1$ that

$$\mathbb{P}(Y_m^m > s, Y_d^m > s \mid Y_{d-1}^m = 0) = \mathbb{P}(Y_m^m > s \mid Y_{d-1}^m = 0) \mathbb{P}(Y_d^m > s \mid Y_{d-1}^m = 0). \quad (29)$$

Since $\mathbb{P}(Y_{d-1}^m = 0) > 0$, the first factor on the right-hand side is positive as

$$\mathbb{P}(Y_m > 1) \mathbb{P}(Y_m^m > s, Y_{d-1}^m = 0) = \mathbb{P}(Y_m > s, Y_{d-1} = 0) = s^{-1} \mathbb{P}(Y_m > 1, Y_{d-1} = 0) > 0,$$

where the last equation follows from the homogeneity of \mathbf{Y} . Thus, equation (29) can be written as

$$\mathbb{P}(Y_d^m > s \mid Y_{d-1}^m = 0) = \frac{\mathbb{P}(Y_m > s, Y_d > s, Y_{d-1} = 0)}{\mathbb{P}(Y_m > s, Y_{d-1} = 0)} = \frac{\mathbb{P}(Y_m > 1, Y_d > 1, Y_{d-1} = 0)}{\mathbb{P}(Y_m > 1, Y_{d-1} = 0)},$$

where we used again the homogeneity of \mathbf{Y} . The right-hand side does therefore not depend on s and thus $\mathbb{P}(Y_d^m > s \mid Y_{d-1}^m = 0) = 0$ for all $s \geq 1$ by taking the limit $s \rightarrow \infty$. Using this, we also obtain

$$\begin{aligned} \mathbb{P}(Y_d > s^{-1}, Y_{d-1} = 0, Y_m > 1) &= s \mathbb{P}(Y_d > 1, Y_{d-1} = 0, Y_m > s) \\ &\leq s \mathbb{P}(Y_d^m > 1, Y_{d-1}^m = 0) \mathbb{P}(Y_m > 1) = 0, \end{aligned}$$

which implies $\mathbb{P}(Y_d^m = 0 \mid Y_{d-1}^m = 0) = 1$ and thus

$$\mathbb{E} [\mathbf{1}\{Y_{d-1}^m = 0\} f(\mathbf{Y}^m)] = \mathbb{E} [\mathbf{1}\{Y_{d-1}^m = 0\} f(\mathbf{Y}_{\setminus d}^m, 0)].$$

Combining this with (28) yields

$$\mathbb{E} [f(\mathbf{Y}^m)] = \mathbb{E} [f(\mathbf{Y}_{\setminus d}^m, Y_{d-1}^m W_d^{d-1})],$$

and by induction we can use the representation (8) for $\mathbf{Y}_{\setminus d}^m$ to conclude the first part of the proof.

For the converse statement, let $\mathbf{Y}^1, \dots, \mathbf{Y}^d$ be random vectors defined as in (8) for independent random variables $\{W_i^j, W_j^i; \{i, j\} \in E\}$, where W_i^j and W_j^i satisfy the duality (5). We first

show that the extremal functions are mutually consistent on the intersections of their domains. For $m, m' \in V$, let $A \subset \mathcal{L}^m \cap \mathcal{L}^{m'}$ be a Borel subset, then

$$\mathbb{P}(\mathbf{Y}^m \in A) = \int_1^\infty u^{-2} \mathbb{P}\left\{u \left(\prod_{e \in \text{ph}(mi; T^m)} W_e \right)_{i \in V} \in A\right\} du, \quad (30)$$

where the empty product is defined as one, and we explicitly specify with respect to which directed tree the path is taken. Note that $\mathbf{Y} \in \mathcal{L}^m \cap \mathcal{L}^{m'}$ implies that all $W_e > 0$ for $e \in \text{ph}(mm'; T^m)$ and $W_{e'} > 0$, where for $e = (i, j)$ the edge $e' = (j, i)$ has reversed orientation. From the duality in (5) we get for any bounded, measurable function $h : [0, \infty) \rightarrow [0, \infty)$

$$\mathbb{E}[h(W_i^j) \mathbf{1}\{W_i^j > 0\}] = \mathbb{E}[h(1/W_j^i) W_j^i]. \quad (31)$$

By swapping the order of integration in (30) we get

$$\begin{aligned} & \mathbb{E}\left[\int_1^\infty u^{-2} \mathbf{1}\left\{u \left(\prod_{e \in E_i} W_e \right)_{i \in V} \in A\right\} du\right] \\ &= \mathbb{E}\left[\int_1^\infty u^{-2} \mathbf{1}\left\{u \left(\prod_{e \in E_i \setminus S} W_e \prod_{e \in E_i \cap S} W_e \right)_{i \in V} \in A\right\} du\right] \\ &= \mathbb{E}\left[\int_1^\infty u^{-2} \mathbf{1}\left\{u \left(\prod_{e \in E_i \setminus S} W_e \prod_{e \in E_i \cap S} 1/W_{e'} \right)_{i \in V} \in A\right\} \prod_{e \in S} W_{e'} du\right] \\ &= \mathbb{E}\left[\int_{1/\prod_{e \in S} W_{e'}}^\infty v^{-2} \mathbf{1}\left\{v \prod_{e \in S} W_{e'} \left(\prod_{e \in E_i \setminus S} W_e \prod_{e \in E_i \cap S} 1/W_{e'} \right)_{i \in V} \in A\right\} dv\right] \\ &= \mathbb{E}\left[\int_{1/\prod_{e \in S} W_{e'}}^\infty v^{-2} \mathbf{1}\left\{v \left(\prod_{e \in \text{ph}(m'i; T^{m'})} W_e \right)_{i \in V} \in A\right\} dv\right] \\ &= \mathbb{E}\left[\int_1^\infty v^{-2} \mathbf{1}\left\{v \left(\prod_{e \in \text{ph}(m'i; T^{m'})} W_e \right)_{i \in V} \in A\right\} dv\right], \end{aligned}$$

where we used the abbreviated notation $E_i := \text{ph}(mi; T^m)$ and $S := \text{ph}(mm'; T^m)$. Here we used independence of the W_e in the first equality, the identity (31) in the second (noting that by the assumptions we made on A the $\mathbf{1}\{W_i^j > 0\}$ in that identity can be dropped), the substitution $u = v \prod_{e \in S} W_{e'}$ in the third equality. The fourth equality follows from elementary considerations upon observing that the edges $e \in T^m$ have the same orientation in $T^{m'}$ whenever $e \notin \text{ph}(mm'; T^m)$ and reversed orientation otherwise. For the last equality recall that by the assumption $A \subset \mathcal{L}^m \cap \mathcal{L}^{m'}$ and by the representation $Y_m^{m'} = P \prod_{e \in \text{ph}(m'm; T^{m'})} W_e$ we have that $v > 1$ and $v > 1/\prod_{e \in S} W_{e'}$ whenever the indicator function is non-zero. This shows that $\mathbb{P}(\mathbf{Y}^{m'} \in A) = \mathbb{P}(\mathbf{Y}^m \in A)$.

We can now define the random vector \mathbf{Y} on \mathcal{L} by

$$\mathbb{P}(\mathbf{Y} \in A) := c \sum_{i=1}^d \mathbb{P}(\mathbf{Y}^i \in A \cap B_i), \quad A \subset \mathcal{L},$$

where $c > 0$ is an appropriate normalizing constant to make this a probability measure and B_1, \dots, B_d define a disjoint partition of the set \mathcal{L} and have the additional property $B_i \subset \mathcal{L}^i, i = 1, \dots, d$.

The \mathbf{Y} defined above is homogeneous as in (3) since all of the \mathbf{Y}^m are homogeneous, and therefore it is a d -dimensional Pareto distribution. Moreover, the conditioned random vector $\mathbf{Y} \mid Y_m > 1$ has the same distribution as \mathbf{Y}^m since for $A \subset \mathcal{L}^m$

$$\mathbb{P}(\mathbf{Y} \in A \mid Y_m > 1) = \frac{\sum_{i=1}^d \mathbb{P}(\mathbf{Y}^i \in A \cap \mathcal{L}^m \cap B_i)}{\sum_{i=1}^d \mathbb{P}(\mathbf{Y}^i \in \mathcal{L}^m \cap B_i)} = \frac{\sum_{i=1}^d \mathbb{P}(\mathbf{Y}^m \in A \cap \mathcal{L}^m \cap B_i)}{\sum_{i=1}^d \mathbb{P}(\mathbf{Y}^m \in \mathcal{L}^m \cap B_i)} = \mathbb{P}(\mathbf{Y}^m \in A),$$

because of the consistency between \mathbf{Y}^m and \mathbf{Y}^i and since for any $i \in V$ the sets $A \cap \mathcal{L}^m \cap B_i$ and $\mathcal{L}^m \cap B_i$ are subsets of $\mathcal{L}^m \cap \mathcal{L}^i$; note further that $\mathbf{Y}^m \in \mathcal{L}^m$ with probability one. Finally, it is readily seen that \mathbf{Y}^m satisfies the global Markov property on T , and thus \mathbf{Y} is an extremal graphical model on T . \square

S.5 Proof of the expression of $\Gamma_{ij}^{(m)}$ in Example 2

Recall the representation of extremal function \mathbf{W}^m for the logistic distribution in Example 2. For $i, j \neq m$, we have

$$\Gamma_{ij}^{(m)} = \text{Var}(\log U_i - \log U_j) = \text{Var}(\log U_i) + \text{Var}(\log U_j).$$

Since the logarithm of a Fréchet distribution is a Gumbel distribution, the result follows after some algebra.

If $i \neq j = m$, we need to compute

$$\Gamma_{ij}^{(m)} = \text{Var}(\log U_i) + \text{Var}(\log U_m).$$

The density of $\log U_m$ is

$$f_{\log U_m}(z) = \frac{e^{-z/\theta+z}}{\theta G(1-\theta)^{1/\theta}} \exp\left\{-G(1-\theta)^{-1/\theta} e^{-z/\theta}\right\}.$$

We can write it as an exponential tilting

$$f(z) = f_{\log U_m}(z) = e^z g(z),$$

where g is the density of Gumbel(location = $-\log G(1-\theta)$, scale = θ) distribution. We need to find the moments $\mathbb{E}(X^k e^X)$, where X is the above Gumbel distribution, $k = 1, 2$.

Recall that the moment generating function of a random variable X is defined as $m(t) = \mathbb{E}[e^{tX}]$. Since derivatives and expectation in this example can be interchanged we obtain for the k th derivative $m^{(k)}(t) = \mathbb{E}[X^k \exp(tX)]$, and thus $\mathbb{E}[X^k e^X] = m^{(k)}(1)$. The moment generating function of a Gumbel(scale = μ , shape = β) is $m(t) = G(1-\beta t)e^{\mu t}$. Hence we obtain after some simple calculations

$$E[X e^X] = -\theta \psi^{(0)}(1-\theta) - \log G(1-\theta)$$

where $\psi^{(0)} = G'/G$ is the digamma function. For the second moment note that for $m(t) = G(1-\beta t)e^{\mu t}$ we have

$$m''(1) = \left(\beta^2 G''(1-\beta) - 2\mu\beta G'(1-\beta t) + \mu^2 G(1-\beta)\right)e^{\mu}.$$

Hence, plugging in $\beta = \theta, \mu = -\log G(1-\theta)$,

$$\begin{aligned} E[X^2 e^X] &= \theta^2 \frac{G''(1-\theta)}{G(1-\theta)} + 2\theta \log G(1-\theta) \frac{G'(1-\theta)}{G(1-\theta)} + \{\log G(1-\theta)\}^2 \\ &= \theta^2 \left(\psi^{(1)}(1-\theta) + \psi^{(0)}(1-\theta)^2\right) + 2\theta \log G(1-\theta) \psi^{(0)}(1-\theta) + \{\log G(1-\theta)\}^2. \end{aligned}$$

where the last equation uses $G''(t)/G(t) = \psi^{(1)}(t) + \psi^{(0)}(t)^2$ for the trigamma function $\psi^{(1)}$. Combining the above expressions some simple algebra yields

$$E[X^2 e^X] - (E[X e^X])^2 = \theta^2 \psi^{(1)}(1-\theta).$$

\square

S.6 Proof of Theorem 2

We give a detailed proof for $\hat{T}_\Gamma^{(m)}$, all other proofs are similar. For an arbitrary tree $T' = (V, E')$ define $\rho_{\Gamma^{(m)}(q)}(T') := \sum_{(i,j) \in E'} \Gamma_{ij}^{(m)}(q)$ and $\hat{\rho}_{\Gamma^{(m)}}(T') := \sum_{(i,j) \in E'} \hat{\Gamma}_{ij}^{(m)}$. By Corollary 1 we know that

$$\min_{T' \neq T} \rho_{\Gamma^{(m)}(0)}(T') - \rho_{\Gamma^{(m)}(0)}(T) > 0.$$

By Proposition 3 we have as $q \rightarrow 0$

$$\min_{T' \neq T} \rho_{\Gamma^{(m)}(q)}(T') - \rho_{\Gamma^{(m)}(q)}(T) \rightarrow \min_{T' \neq T} \rho_{\Gamma^{(m)}(0)}(T') - \rho_{\Gamma^{(m)}(0)}(T) > 0,$$

hence there exists a $1 \geq q^* > 0$ such that

$$\min_{T' \neq T} \rho_{\Gamma^{(m)}(q)}(T') - \rho_{\Gamma^{(m)}(q)}(T) > 0 \quad \forall q \in [0, q^*].$$

Now for $k/n \rightarrow q \in [0, q^*]$ Theorem 1 implies that

$$\min_{T' \neq T} \hat{\rho}_{\Gamma^{(m)}}(T') - \hat{\rho}_{\Gamma^{(m)}}(T) = \min_{T' \neq T} \rho_{\Gamma^{(m)}(q)}(T') - \rho_{\Gamma^{(m)}(q)}(T) + o_{\mathbb{P}}(1),$$

which yields

$$P\left(\min_{T' \neq T} \hat{\rho}_{\Gamma^{(m)}}(T') - \hat{\rho}_{\Gamma^{(m)}}(T) > 0\right) \rightarrow 1.$$

The claim for $\hat{T}_\Gamma^{(m)}$ follows. For the corresponding result on \hat{T}_Γ^w we apply Corollary 2 instead of Corollary 1. To prove the consistency for \hat{T}_χ we use (15) instead of Theorem 1, Proposition 5 instead of Corollary 1, and note that $\chi_{ij}(q) \rightarrow \chi_{ij}$ as $q \rightarrow 0$ follows from (2) since by connectedness of the tree $\chi_{ij} \neq 0$ for all $i \neq j$ and the definition of χ_{ij} . \square

S.7 Proofs of Proposition 3 and Theorem 1

We begin by discussing several preliminaries that will be useful in both proofs.

For notational convenience we define the random variables $U_i := 1 - F_i(X_i)$. Denote the joint distribution of $\mathbf{U} := (U_1, \dots, U_d)$ by C and for $I \subset V$ with $|I| \in \{2, 3\}$ let

$$R_I(\mathbf{x}) := \lim_{q \rightarrow 0} q^{-1} \mathbb{P}(F_I(\mathbf{X}_I) \geq 1 - q\mathbf{x}_I).$$

Those limits exist by condition (B) and simple manipulations involving the inclusion-exclusion formula. Note that R can be represented as linear combination of the functions ℓ_I for various $I \subset \{1, \dots, d\}$ and is thus homogeneous of order 1.

Since

$$\Gamma_{i,j}^{(m)} = \text{Var}(\log(1/Y_i^m) - \log(1/Y_j^m))$$

we have

$$\Gamma_{i,j}^{(m)} = e_i^{(m),2} + e_j^{(m),2} - 2e_{i,j}^{(m)} - \left(e_i^{(m),1} - e_j^{(m),1}\right)^2 \quad (32)$$

where

$$\begin{aligned} e_{i,j}^{(m)} &= \mathbb{E}[\log(1/Y_i^m) \log(1/Y_j^m)] \\ e_i^{(m),\ell} &= \mathbb{E}[(\log(1/Y_i^m))^\ell] \end{aligned}$$

For the pre-asymptotic versions, define the random vectors $\mathbf{U}^m(q)$ with distribution on

$$\mathcal{D}^m(q) := [0, 1]^{m-1} \times [0, q] \times [0, 1]^{d-m}$$

given by

$$\mathbb{P}(\mathbf{U}^m(q) \in A) = q^{-1} \mathbb{P}(\mathbf{U} \in A \cap \mathcal{D}^m(q))$$

With this notation the pre-asymptotic variogram can be represented as

$$\begin{aligned} \Gamma_{ij}^{(m)}(q) &= \text{Var} \left(-\log\{U_i^m(q)/q\} + \log\{U_j^m(q)/q\} \right) \\ &= e_i^{(m),2}(q) + e_j^{(m),2}(q) - 2e_{i,j}^{(m)}(q) - \left(e_i^{(m),1}(q) - e_j^{(m),1}(q) \right)^2 \end{aligned} \quad (33)$$

with

$$\begin{aligned} e_{i,j}^{(m)}(q) &= \mathbb{E}[\log(U_i^m(q)/q) \log(U_j^m(q)/q)] \\ e_i^{(m),\ell}(q) &= \mathbb{E}[(-\log(U_i^m(q)/q))^\ell]. \end{aligned}$$

The quantities above have alternative representations which we will use in the following proof. First note that for $i \neq m$ we have

$$e_i^{(m),\ell} = \int_0^1 \frac{R_{i,m}(x,1) \ell(-\log x)^{\ell-1}}{x} dx + \int_1^\infty \frac{(R_{i,m}(x,1) - 1) \ell(-\log x)^{\ell-1}}{x} dx, \quad (34)$$

$$e_i^{(m),\ell}(q) = \int_0^1 \frac{q^{-1} C_{i,m}(qx, q) \ell(-\log x)^{\ell-1}}{x} dx + \int_1^{q^{-1}} \frac{(q^{-1} C_{i,m}(qx, q) - 1) \ell(-\log x)^{\ell-1}}{x} dx. \quad (35)$$

For the next representations assume that i, j, m are all different. Then

$$e_{i,j}^{(j)} = \int_0^1 \int_0^1 \frac{R_{i,j}(x, y)}{xy} dx dy + \int_0^1 \int_1^\infty \frac{R_{i,j}(x, y) - y}{xy} dx dy, \quad (36)$$

$$e_{i,j}^{(j)}(q) = \int_0^1 \int_0^1 \frac{C_{i,j}(qx, qy)}{qxy} dx dy + \int_0^1 \int_1^{q^{-1}} \frac{C_{i,j}(qx, qy) - C_{i,j}(1, qy)}{qxy} dx dy, \quad (37)$$

and

$$\begin{aligned} e_{i,j}^{(m)} &= \int_0^1 \int_0^1 \frac{R_{i,j,m}(x, y, 1)}{xy} dx dy \\ &+ \int_0^1 \int_1^\infty \frac{R_{i,j,m}(x, y, 1) - R_{i,j,m}(\infty, y, 1)}{xy} dx dy \\ &+ \int_1^\infty \int_0^1 \frac{R_{i,j,m}(x, y, 1) - R_{i,j,m}(x, \infty, 1)}{xy} dx dy \\ &+ \int_1^\infty \int_1^\infty \frac{R_{i,j,m}(x, y, 1) - R_{i,j,m}(\infty, y, 1) - R_{i,j,m}(x, \infty, 1) + R_{i,j,m}(\infty, \infty, 1)}{xy} dx dy \end{aligned} \quad (38)$$

as well as

$$\begin{aligned} e_{i,j}^{(m)}(q) &= \int_0^1 \int_0^1 \frac{C_{i,j,m}(qx, qy, q)}{qxy} dx dy \\ &+ \int_0^1 \int_1^{1/q} \frac{C_{i,j,m}(qx, qy, q) - C_{i,j,m}(1, qy, q)}{qxy} dx dy \\ &+ \int_1^{1/q} \int_0^1 \frac{C_{i,j,m}(qx, qy, q) - C_{i,j,m}(qx, 1, q)}{qxy} dx dy \\ &+ \int_1^{1/q} \int_1^{1/q} \frac{C_{i,j,m}(qx, qy, q) - C_{i,j,m}(1, qy, q) - C_{i,j,m}(qx, 1, q) + C_{i,j,m}(1, 1, q)}{qxy} dx dy. \end{aligned} \quad (39)$$

Next we discuss similar representations for the empirical version of the extremal variogram. Define the random variables $U_{ti} := 1 - F_i(X_{ti})$ (here X_{ti} denotes the i 'th entry of the vector \mathbf{X}_t) and the vectors $\mathbf{U}_t := (U_{t1}, \dots, U_{td})^\top$. Let $R(\mathbf{x}) := \Lambda([\mathbf{1}/\mathbf{x}, \infty))$ and denote by \hat{F}_i the empirical distribution function U_{1i}, \dots, U_{ni} . Define the vector $\hat{\mathbf{F}}^-(\mathbf{x}) := (\hat{F}_1^-(x_1), \dots, \hat{F}_d^-(x_d))$, the function

$$\hat{C}^\circ(\mathbf{x}) := \frac{1}{n} \sum_{i=1}^n I\{U_{t1} \leq x_1, \dots, U_{td} \leq x_d\} \quad (40)$$

and $\hat{C}(k\mathbf{x}/n) := \hat{C}^\circ(\hat{\mathbf{F}}^-(k\mathbf{x}/n))$. Introduce the notation

$$\hat{R}_I(\mathbf{x}) := \frac{n}{k} \hat{C}_I(k\mathbf{x}/n).$$

Note that the estimator $\hat{\Gamma}^{(m)}$ depends only on the marginal ranks of X_{ti} ; thus we have almost surely

$$\begin{aligned} \hat{\Gamma}_{i,j}^{(m)} &= \widehat{\text{Var}}\left(\log(\hat{F}_i(U_{ti})) - \log(\hat{F}_j(U_{tj})) : \hat{F}_m(U_{tm}) \leq \frac{k}{n}\right) \\ &= \widehat{\text{Var}}\left(-\log(n\hat{F}_i(U_{ti})/k) + \log(n\hat{F}_j(U_{tj})/k) : \hat{F}_m(U_{tm}) \leq \frac{k}{n}\right). \end{aligned}$$

Now observe the following representation

$$\hat{\Gamma}_{i,j}^{(m)} = \hat{e}_i^{(m),2} + \hat{e}_j^{(m),2} - 2\hat{e}_{i,j}^{(m)} - \left(\hat{e}_i^{(m),1} - \hat{e}_j^{(m),1}\right)^2 \quad (41)$$

where

$$\begin{aligned} \hat{e}_i^{(m),\ell} &:= \frac{1}{k} \sum_{t=1}^n \left\{ -\log\left(\frac{n\hat{F}_i(U_{ti})}{k}\right) \right\}^\ell I\{\hat{F}_m(U_{tm}) \leq k/n\}, \quad \ell = 1, 2 \\ \hat{e}_{ij}^{(m)} &:= \frac{1}{k} \sum_{t=1}^n \log\left(\frac{n\hat{F}_j(U_{tj})}{k}\right) \log\left(\frac{n\hat{F}_i(U_{ti})}{k}\right) I\{\hat{F}_m(U_{tm}) \leq k/n\}. \end{aligned}$$

The quantities above have alternative representations which we will use frequently. The exact form of those representations depends on whether $m \in \{i, j\}$ or $m \notin \{i, j\}$ and those two cases will be considered separately.

We start with the case $m \in \{i, j\}$. Assume without loss of generality that $j = m$. Then

$$\begin{aligned} \hat{e}_{ij}^{(j)} &= \int_{1/k}^1 \int_{1/k}^1 \frac{\hat{R}_{ij}(x, y)}{xy} dx dy + \int_{1/k}^1 \int_1^{n/k} \frac{\hat{R}_{ij}(x, y) - \hat{R}_{ij}(n/k, y)}{xy} dx dy + O((\log n)^2/k), \quad (42) \\ \hat{e}_i^{(j),\ell} &= \int_{1/k}^1 \frac{\hat{R}_{ij}(x, 1)\ell(-\log x)^{\ell-1}}{x} dx + \int_1^{n/k} \frac{(\hat{R}_{ij}(x, 1) - 1)\ell(-\log x)^{\ell-1}}{x} dx + O((\log n)^2/k). \end{aligned} \quad (43)$$

We also note that

$$\begin{aligned} \hat{e}_i^{(i),\ell} &= \frac{1}{k} \sum_{t=1}^n \left\{ -\log\left(\frac{n\hat{F}_i(U_{ti})}{k}\right) \right\}^\ell I\{\hat{F}_i(U_{ti}) \leq k/n\} = \frac{1}{k} \sum_{t=1}^k \{-\log(t/k)\}^\ell \\ &= \int_0^1 \{\log(1/x)\}^\ell dx + o(1) = \mathbb{E}[(\log Y_i^{(i)})^\ell] + o(1) \end{aligned}$$

where we used that $Y_i^{(i)}$ is unit Pareto and the difference between the integral and the sum is $o(1)$ by a standard Riemann approximation. When $m \notin \{i, j\}$ we have

$$\begin{aligned}
\hat{e}_{i,j}^{(m)} &= \int_{1/k}^1 \int_{1/k}^1 \frac{\widehat{R}_{i,j,m}(x, y, 1)}{xy} dx dy \\
&+ \int_{1/k}^1 \int_1^{n/k} \frac{\widehat{R}_{i,j,m}(x, y, 1) - \widehat{R}_{i,j,m}(\infty, y, 1)}{xy} dx dy \\
&+ \int_1^{n/k} \int_{1/k}^1 \frac{\widehat{R}_{i,j,m}(x, y, 1) - \widehat{R}_{i,j,m}(x, \infty, 1)}{xy} dx dy \\
&+ \int_1^{n/k} \int_1^{n/k} \frac{\widehat{R}_{i,j,m}(x, y, 1) - \widehat{R}_{i,j,m}(\infty, y, 1) - \widehat{R}_{i,j,m}(x, \infty, 1) + 1}{xy} dx dy + O((\log n)^2/k)
\end{aligned} \tag{44}$$

while the representation for $\hat{e}_i^{(m),\ell}$ does not change.

All representations defined above will be established in section S.7.3. After this preparation, we proceed to proving the main asymptotic results.

S.7.1 Proof of Proposition 3

Observe that condition (B) implies

$$\sup_{2 \leq |I| \leq 3} \sup_{\mathbf{x} \in [0,1]^{|I|}} \left| \frac{1}{q} C_I(q\mathbf{x}) - R_I(\mathbf{x}) \right| = O(q^\xi), \quad (q \rightarrow 0), \tag{45}$$

and we can rewrite (T) for any $I = \{i, m\}$ as

$$\begin{aligned}
|R_I(T, 1) - 1| &= \mathbb{P}(Y_i^m \leq 1/T) \\
&= \int_1^\infty x^{-2} \mathbb{P}(x W_i^m \leq 1/T) dx \\
&= \int_1^\infty x^{-2} \mathbb{P}(1/W_i^m \geq xT) dx \\
&\leq \mathbb{E}(W_i^m)^{-\gamma} T^{-\gamma} \int_1^\infty x^{-2-\gamma} dx = O(T^{-\gamma}),
\end{aligned} \tag{46}$$

by Markov's inequality.

We begin by proving some useful technical results: under (45) and (46) we have for any $0 < \delta < 1$ such that $(1 - \delta)\xi - \delta > 0$

$$\sup_{2 \leq |I| \leq 3} \sup_{\mathbf{x} \in [0, q^{-\delta}]^{|I|-1} \times [0,1]} \left| \frac{1}{q} C_I(q\mathbf{x}) - R_I(\mathbf{x}) \right| = O(q^{(1-\delta)\xi - \delta}) \tag{47}$$

$$\sup_{2 \leq |I| \leq 3} \sup_{\mathbf{x} \in [q^{-\delta}, q^{-1}]^{|I|-1} \times [0,1]} \left| \frac{1}{q} C_I(q\mathbf{x}) - R_I(\mathbf{x}) \right| = O(q^{(1-\delta)\xi - \delta} + q^{\gamma\delta}) \tag{48}$$

$$\sup_{|I|=3} \sup_{\mathbf{x} \in [q^{-\delta}, q^{-1}] \times [0, q^{-\delta}] \times [0,1]} \left| \frac{1}{q} C_I(q\mathbf{x}) - R_I(\mathbf{x}) \right| = O(q^{(1-\delta)\xi - \delta} + q^{\gamma\delta}) \tag{49}$$

Note that combining the above bounds and setting $\delta = \xi/(\xi + \gamma + 1)$ implies

$$\sup_{2 \leq |I| \leq 3} \sup_{\mathbf{x} \in [0, q^{-1}]^{|I|-1} \times [0,1]} \left| \frac{1}{q} C_I(q\mathbf{x}) - R_I(\mathbf{x}) \right| = O(q^{\xi\gamma/(\xi+\gamma+1)}), \quad (q \rightarrow 0) \tag{50}$$

The key difference to (45) is that some components of \mathbf{x} are now allowed to vary over a growing set as $q \rightarrow 0$. The price for this generalization is a strictly smaller power of q in the corresponding upper bound.

Next we derive a general bound on R . Let $I \subset \{1, \dots, d\}$ with $|I| = 3$ be arbitrary. Note that R_I can be seen as the distribution function of a measure on $[0, \infty)^3$ and that $R_I(\infty, \infty, x) = x$, and thus slightly abusing notation we have

$$\begin{aligned} \sup_{x \geq 1, y \in [0, \infty], z \in [0, 1]} x^\gamma \left| R_I(x, y, z) - R_I(\infty, y, z) \right| &= \sup_{x \geq 1, y \in [0, \infty], z \in [0, 1]} x^\gamma R_I((x, \infty) \times [0, y] \times [0, z]) \\ &= \sup_{x \geq 1} x^\gamma R_I((x, \infty) \times [0, \infty] \times [0, 1]) < \infty, \end{aligned} \quad (51)$$

where the finiteness of the last display follows by (46). In particular this implies

$$\sup_{x \geq q^{-\delta}, y \in [0, \infty], z \in [0, 1]} \left| R_I(x, y, z) - R_I(\infty, y, z) \right| = O(q^{\gamma\delta}). \quad (52)$$

For a proof of (47), note that by (45) and homogeneity of R we have for $\|\mathbf{x}\|_\infty \leq q^{-\delta}$

$$\frac{1}{q} C_I(q\mathbf{x}) = \frac{1}{q} C_I(q^{1-\delta} q^\delta \mathbf{x}) = \frac{q^{1-\delta}}{q} \left\{ R_I(q^\delta \mathbf{x}) + O(q^{(1-\delta)\xi}) \right\} = R_I(\mathbf{x}) + O(q^{(1-\delta)\xi-\delta}).$$

For a proof of (49) observe that have for $q^{-1} \geq x \geq q^{-\delta}, y \leq q^{-\delta}, I = (i_1, i_2, i_3)$

$$\begin{aligned} \frac{1}{q} C_I(1, qy, qz) &\geq \frac{1}{q} C_I(qx, qy, qz) \geq \frac{1}{q} C(q^{1-\delta}, qy, qz) = \frac{1}{q} C_I(qq^{-\delta}, qy, qz) \\ &= R_I(q^{-\delta}, y, z) + O(q^{(1-\delta)\xi-\delta}) = R_I(\infty, y, z) + O(q^{(1-\delta)\xi-\delta} + q^{\gamma\delta}) \\ &= \frac{1}{q} C_I(1, qy, qz) + O(q^{(1-\delta)\xi-\delta} + q^{\gamma\delta}) \end{aligned}$$

where the last equality follows by (47) applied with $I = (i_2, i_3)$, the second equality follows by (47), the third equality follows by (52) and all O terms are uniform in $q^{-1} \geq x \geq q^{-\delta}, y \leq q^{-\delta}, I = (i_1, i_2, i_3)$. This implies

$$\sup_{|I|=3} \sup_{\mathbf{x} \in [q^{-\delta}, q^{-1}] \times [0, q^{-\delta}] \times [0, 1]} \left| \frac{1}{q} C_I(qx, qy, qz) - \frac{1}{q} C_I(1, qy, qz) \right| = O(q^{(1-\delta)\xi-\delta} + q^{\gamma\delta}) \quad (53)$$

and also

$$\sup_{|I|=3} \sup_{\mathbf{x} \in [q^{-\delta}, q^{-1}] \times [0, q^{-\delta}] \times [0, 1]} \left| \frac{1}{q} C_I(qx, qy, qz) - R_I(\infty, y, z) \right| = O(q^{(1-\delta)\xi-\delta} + q^{\gamma\delta}).$$

Combined with (52) this completes the proof of (49).

The proof of (48) is similar. Indeed we have for $\mathbf{x} \in [q^{-\delta}, \infty)^{|I|-1} \times [0, 1]$

$$x_3 \geq R_I(\mathbf{x}) \geq R_I(q^{-\delta}, q^{-\delta}, x_3) = R_I(\infty, q^{-\delta}, x_3) + O(q^{\gamma\delta}) = x_3 + O(q^{\gamma\delta})$$

where (52) is applied twice: first with $y = q^{-\delta}$ and second with $I = (i_1, i_2)$. By (47) and the bound above

$$x_3 \geq \frac{1}{q} C_I(q\mathbf{x}) \geq \frac{1}{q} C_I(qq^{-\delta}, qq^{-\delta}, x_3) = R_I(q^{-\delta}, q^{-\delta}, x_3) + O(q^{(1-\delta)\xi-\delta}) = x_3 + O(q^{(1-\delta)\xi-\delta} + q^{\gamma\delta}).$$

Combining the two chains of inequalities above we find that $q^{-1} C_I(q\mathbf{x}) = x_3 + O(q^{(1-\delta)\xi-\delta} + q^{\gamma\delta})$ and $R_I(\mathbf{x}) = x_3 + O(q^{\gamma\delta})$ implies (48).

We will now show that $e_i^{(m),\ell}(q) \rightarrow e_i^{(m),\ell}$, $e_{i,j}^{(m)}(q) \rightarrow e_{i,j}^{(m)}$ and $e_{i,m}^{(m)}(q) \rightarrow e_{i,m}^{(m)}$. Combined with the representations in (32), (33) this will complete the proof of Proposition 3.

Proof of $e_i^{(m),\ell}(q) \rightarrow e_i^{(m),\ell}$ To keep the notation simple we only consider the case $\ell = 1$, the case $\ell = 2$ follows by exactly the same arguments. We have

$$0 \leq \int_0^{q^\xi} \frac{1}{x} \frac{1}{q} C_{i,m}(qx, q) dx \leq \int_0^{q^\xi} \frac{1}{xq} xq dx = q^\xi$$

and

$$\begin{aligned} \int_{q^\xi}^1 \frac{1}{x} \frac{1}{q} C_{i,m}(qx, q) dx &= \int_{q^\xi}^1 \frac{1}{x} \left\{ R_{i,m}(x, 1) + O(q^\xi) \right\} dx = \int_{q^\xi}^1 \frac{1}{x} R_{i,m}(x, 1) dx + O(q^\xi |\log q|) \\ &= \int_0^1 \frac{1}{x} R_{i,m}(x, 1) dx + O(q^\xi |\log q|) \end{aligned}$$

where the last line follows since $0 \leq \frac{1}{x} R_{i,m}(x, 1) = R_{i,m}(1, 1/x) \leq R_{i,m}(1, \infty) = 1$. Next observe that by (50)

$$\int_1^{q^{-1}} \frac{1}{x} \left\{ \frac{1}{q} C_{i,m}(qx, q) - 1 \right\} dx - \int_1^{q^{-1}} \frac{1}{x} \left\{ R_{i,m}(x, 1) - 1 \right\} dx = O(q^{\gamma\xi/(\gamma+\xi+1)} |\log q|).$$

The claim follows by combining this with (34), (35) and the fact that by (46)

$$\int_{q^{-1}}^\infty \frac{1}{x} \left\{ R_{i,m}(x, 1) - 1 \right\} dx = o(1).$$

Proof of $e_{i,j}^{(m)}(q) \rightarrow e_{i,j}^{(m)}$ and $e_{i,m}^{(m)}(q) \rightarrow e_{i,m}^{(m)}$

Since the proof of $e_{i,m}^{(m)}(q) \rightarrow e_{i,m}^{(m)}$ is similar but simpler we will only provide details for $e_{i,j}^{(m)}(q) \rightarrow e_{i,j}^{(m)}$. For the sake of a lighter notation we will drop the index i, j, m from C, R in all calculations that follow.

Fix $\alpha > \xi$. Then

$$\int_0^1 \int_0^1 \frac{1}{xy} \frac{1}{q} C(qx, qy, q) dx dy = \int_{[q^\alpha, 1]^2} \frac{1}{xy} \frac{1}{q} C(qx, qy, q) dx dy + \int_{([q^\alpha, 1]^2)^c} \frac{1}{xy} \frac{1}{q} C(qx, qy, q) dx dy$$

First, by (45),

$$\int_{[q^\alpha, 1]^2} \frac{1}{xy} \frac{1}{q} C(qx, qy, q) dx dy = \int_{[q^\alpha, 1]^2} \frac{1}{xy} R(x, y, 1) dx dy + O((\log q)^2 q^\xi).$$

Second, by the upper Fréchet–Hoeffding bound

$$\begin{aligned} 0 &\leq \int_{([q^\alpha, 1]^2)^c} \frac{1}{xy} \frac{1}{q} C(qx, qy, q) dx dy \leq \left(\int_0^{q^\alpha} \int_0^1 + \int_0^1 \int_0^{q^\alpha} \right) \frac{1}{xy} \frac{1}{q} C(qx, qy, q) dx dy \\ &\leq 2 \int_0^{q^\alpha} \int_0^1 \frac{x \wedge y}{xy} dx dy = o(q^\xi) \end{aligned}$$

where the last line follows since

$$\int_0^{q^\alpha} \int_0^1 \frac{x \wedge y}{xy} dx dy = \int_0^{q^\alpha} \frac{1}{y} \left(\int_0^y \frac{x}{x} dx + \int_y^1 \frac{y}{x} dx \right) dy = \int_0^{q^\alpha} 1 - \log(y) dy.$$

Lastly, since $R(x, y, 1) \leq x \wedge y$, we have proved

$$\int_0^1 \int_0^1 \frac{1}{xy} \frac{1}{q} C(qx, qy, q) dx dy = \int_0^1 \int_0^1 \frac{1}{xy} R(x, y, 1) dx dy + O(q^\xi (\log q)^2). \quad (54)$$

Next consider the decomposition

$$\begin{aligned} & \int_0^1 \int_1^{1/q} \frac{1}{xy} \frac{1}{q} \{C(qx, qy, q) - C(1, qy, q)\} dx dy \\ &= \left(\int_0^{q^\alpha} \int_1^{1/q} + \int_{q^\alpha}^1 \int_1^{1/q} \right) \frac{1}{xy} \frac{1}{q} \{C(qx, qy, q) - C(1, qy, q)\} dx dy. \end{aligned}$$

Noting that

$$\left| C(qx, qy, q) - C(1, qy, q) \right| \leq qy$$

the first term can be bounded as follows

$$0 \leq \int_0^{q^\alpha} \int_1^{1/q} \frac{1}{xy} \frac{1}{q} \{C(1, qy, q) - C(qx, qy, q)\} dx dy \leq \int_0^{q^\alpha} \int_1^{1/q} \frac{1}{x} dx dy = q^\alpha |\log(q)|.$$

Similarly we have

$$0 \leq \int_0^{q^\alpha} \int_1^{1/q} \frac{1}{xy} \{R(\infty, y, 1) - R(x, y, 1)\} dx dy \leq \int_0^{q^\alpha} \int_1^{1/q} \frac{1}{x} dx dy = q^\alpha |\log(q)|.$$

Next, by (50)

$$\begin{aligned} \int_{q^\alpha}^1 \int_1^{q^{-1}} \frac{1}{xy} \frac{1}{q} \{C(qx, qy, q) - C(1, qy, q)\} dx dy &= \int_{q^\alpha}^1 \int_1^{q^{-1}} \frac{1}{xy} \{R(x, y, 1) - R(\infty, y, 1)\} dx dy \\ &+ O(q^{\gamma\xi/(\gamma+\xi+1)} (\log q)^2). \end{aligned}$$

By (51) we have

$$\left| \int_{q^\alpha}^1 \int_{q^{-1}}^\infty \frac{1}{xy} \{R(x, y, 1) - R(\infty, y, 1)\} dx dy \right| \leq |\log q| O(1) \int_{q^{-1}}^\infty x^{-1-\gamma} dx = O(|\log q| q^\gamma).$$

Finally, since by (51)

$$\left| R(x, y, 1) - R(\infty, y, 1) \right| \leq K(y \wedge x^{-\gamma})$$

we have

$$\int_0^{q^\alpha} \int_{q^{-1}}^\infty \frac{1}{xy} \{R(x, y, 1) - R(\infty, y, 1)\} dx dy = O(q^\alpha |\log q|).$$

In summary, we have proved

$$\begin{aligned} & \int_0^1 \int_1^{1/q} \frac{1}{xy} \frac{1}{q} \{C(qx, qy, q) - C(1, qy, q)\} dx dy \\ &= \int_0^1 \int_1^\infty \frac{1}{xy} \{R(x, y, 1) - R(\infty, y, 1)\} dx dy + o(1) \quad (55) \end{aligned}$$

Next observe that by (50)

$$\begin{aligned} & \int_1^{q^{-1}} \int_1^{q^{-1}} \frac{1}{xy} \frac{1}{q} \{C(qx, qy, q) - C(1, qy, q) - C(qx, 1, q) + C(1, 1, q)\} dx dy \\ &= \int_1^{q^{-1}} \int_1^{q^{-1}} \frac{R(x, y, 1) - R(\infty, y, 1) - R(x, \infty, 1) + R(\infty, \infty, 1)}{xy} dx dy + (\log q)^2 O(q^{\gamma\xi/(\gamma+\xi+1)}). \end{aligned} \quad (56)$$

Furthermore, (51) implies that

$$\begin{aligned} \sup_{x,y \geq 1} x^\gamma \left| R(x, y, 1) - R(\infty, y, 1) - R(x, \infty, 1) + R(\infty, \infty, 1) \right| &< \infty \\ \sup_{x,y \geq 1} y^\gamma \left| R(x, y, 1) - R(\infty, y, 1) - R(x, \infty, 1) + R(\infty, \infty, 1) \right| &< \infty \end{aligned}$$

to see this apply the triangle inequality and use (51) on both resulting parts noting that $y = \infty$ is explicitly allowed in (51). Thus

$$\begin{aligned} \left(\int_1^\infty \int_1^\infty - \int_1^{q^{-1}} \int_1^{q^{-1}} \right) \frac{\left| R(x, y, 1) - R(\infty, y, 1) - R(x, \infty, 1) + R(\infty, \infty, 1) \right|}{xy} dx dy \\ \leq K \left(\int_1^\infty \int_1^\infty - \int_1^{q^{-1}} \int_1^{q^{-1}} \right) \frac{x^{-\gamma} \wedge y^{-\gamma}}{xy} dx dy = o(1) \end{aligned} \quad (57)$$

Thus combining (54)- (57) with (38) and (39) the claim follows. \square

S.7.2 Proof of Theorem 1

A close look at the proof that follows shows that it continues to hold under the following high-level condition: there exists a $\beta > 0$ such that for any $I \subset V$ with $|I| \leq 3$ such that

$$\sup_{\mathbf{x} \in [0,1]^{|I|}} \frac{n}{k} \left| \hat{C}_I(k\mathbf{x}/n) - C_I(k\mathbf{x}/n) \right| = O_{\mathbb{P}}(k^{-\beta}). \quad (58)$$

For independent observations this is true with $\beta = 1/2$ as we will establish below. Under suitable short-range dependence such as α -mixing with sufficiently fast decay of the mixing coefficients or conditions on physical dependence measures this type of result can be established by the usual chaining arguments. Note that process convergence is explicitly not required and the rate can be slower than the typical $k^{-1/2}$ rate that is expected when process convergence does hold. We omit details for the sake of brevity.

We will show later that there exists a $\psi > 0$ such that for all $I \subset V$ with $2 \leq |I| \leq 3$ and any fixed $0 \leq T < \infty$

$$\sup_{\mathbf{x} \in [0, n/k]^{|I|-1} \times [0, T]} \left| \hat{R}_I(\mathbf{x}) - \frac{n}{k} C_I(k\mathbf{x}/n) \right| = O_P(n^{-\psi}). \quad (59)$$

Note that this differs from common results on convergence of estimators of R because some arguments are now allowed to vary over growing sets.

Now recall the representation for $e_i^{(m),\ell}(q)$ given in (35) and apply it with $q = k/n$ to obtain

$$\begin{aligned} e_i^{(m),\ell}(k/n) &= \int_0^1 \frac{(n/k) C_{i,m}(kx/n, k/n) \ell(-\log x)^{\ell-1}}{x} dx \\ &\quad + \int_1^{n/k} \frac{((n/k) C_{i,m}(kx/n, k/n) - 1) \ell(-\log x)^{\ell-1}}{x} dx. \end{aligned}$$

Further note that by the bound $(n/k) C_{i,m}(kx/n, k/n) \leq x$ we also have

$$\begin{aligned} e_i^{(m),\ell}(k/n) &= \int_{1/k}^1 \frac{(n/k) C_{i,m}(kx/n, k/n) \ell(-\log x)^{\ell-1}}{x} dx \\ &\quad + \int_1^{n/k} \frac{((n/k) C_{i,m}(kx/n, k/n) - 1) \ell(-\log x)^{\ell-1}}{x} dx + o(1). \end{aligned}$$

Combining this with (43) and (59) we find that

$$\begin{aligned} \left| \hat{e}_i^{(m),\ell} - e_i^{(m),\ell}(k/n) \right| &\leq \int_{1/k}^{n/k} \frac{\ell |\log x|^{\ell-1}}{x} dx \sup_{x \in [0, n/k]} \left| \hat{R}_{i,m}(x, 1) - \frac{n}{k} C_{i,m}(kx/n, k/n) \right| + o(1) \\ &= O_{\mathbb{P}}(n^{-\psi} (\log n)^\ell) + o(1) = o_{\mathbb{P}}(1). \end{aligned}$$

It now remains to show that for $k/n \rightarrow q \in [0, 1)$ we have $e_i^{(m),\ell}(k/n) \rightarrow e_i^{(m),\ell}(q)$. For $q > 0$ this statement follows by uniform continuity of $C_{i,m}$ combined with the dominated convergence theorem after noting that $|(n/k)C_{i,m}(kx/n, k/n)| \leq x$ and after noting that in this case the integration range $[1, n/k]$ remains bounded. For $q = 0$ this statement was established in the proof of Proposition 3 (there we considered a general $q \rightarrow 0$, replace that q by k/n). In summary, we proved that for $k/n \rightarrow q \in [0, 1)$

$$\hat{e}_i^{(m),\ell} = e_i^{(m),\ell}(q) + o_{\mathbb{P}}(1). \quad (60)$$

The proof of $\hat{e}_{ij}^{(m)} = e_{ij}^{(m)}(k/n) + o_{\mathbb{P}}(1)$ is similar, and for the sake of brevity we only treat the more complicated case i, j, m all different. Apply the representation in (39) with $q = k/n$ and note that

$$\begin{aligned} e_{i,j}^{(m)}\left(\frac{k}{n}\right) &= \int_0^1 \int_0^1 \frac{n}{k} \frac{C_{i,j,m}\left(\frac{kx}{n}, \frac{ky}{n}, \frac{k}{n}\right)}{xy} dx dy \\ &\quad + \int_0^1 \int_1^{n/k} \frac{n}{k} \frac{C_{i,j,m}\left(\frac{kx}{n}, \frac{ky}{n}, \frac{k}{n}\right) - C_{i,j,m}\left(1, \frac{ky}{n}, \frac{k}{n}\right)}{xy} dx dy \\ &\quad + \int_1^{n/k} \int_0^1 \frac{n}{k} \frac{C_{i,j,m}\left(\frac{kx}{n}, \frac{ky}{n}, \frac{k}{n}\right) - C_{i,j,m}\left(\frac{kx}{n}, 1, \frac{k}{n}\right)}{(n/k)xy} dx dy \\ &\quad + \int_1^{n/k} \int_1^{n/k} \frac{n}{k} \frac{C_{i,j,m}\left(\frac{kx}{n}, \frac{ky}{n}, \frac{k}{n}\right) - C_{i,j,m}\left(1, \frac{ky}{n}, \frac{k}{n}\right) - C_{i,j,m}\left(\frac{kx}{n}, 1, \frac{k}{n}\right) + C_{i,j,m}\left(1, 1, \frac{k}{n}\right)}{xy} dx dy \\ &= \int_{1/k}^1 \int_{1/k}^1 \frac{n}{k} \frac{C_{i,j,m}\left(\frac{kx}{n}, \frac{ky}{n}, \frac{k}{n}\right)}{xy} dx dy \\ &\quad + \int_{1/k}^1 \int_1^{n/k} \frac{n}{k} \frac{C_{i,j,m}\left(\frac{kx}{n}, \frac{ky}{n}, \frac{k}{n}\right) - C_{i,j,m}\left(1, \frac{ky}{n}, \frac{k}{n}\right)}{xy} dx dy \\ &\quad + \int_1^{n/k} \int_{1/k}^1 \frac{n}{k} \frac{C_{i,j,m}\left(\frac{kx}{n}, \frac{ky}{n}, \frac{k}{n}\right) - C_{i,j,m}\left(\frac{kx}{n}, 1, \frac{k}{n}\right)}{xy} dx dy \\ &\quad + \int_1^{n/k} \int_1^{n/k} \frac{n}{k} \frac{C_{i,j,m}\left(\frac{kx}{n}, \frac{ky}{n}, \frac{k}{n}\right) - C_{i,j,m}\left(1, \frac{ky}{n}, \frac{k}{n}\right) - C_{i,j,m}\left(\frac{kx}{n}, 1, \frac{k}{n}\right) + C_{i,j,m}\left(1, 1, \frac{k}{n}\right)}{xy} dx dy \\ &\quad + o(1) \end{aligned}$$

where the equality follows from the bounds $C_{i,j,m}(qx, qy, q)/q \leq x \wedge y$. Combining this with (44) and (59) we find that

$$\begin{aligned} &\left| \hat{e}_{i,j}^{(m)} - e_{i,j}^{(m)}(k/n) \right| \\ &\leq \int_{1/k}^{n/k} \int_{1/k}^{n/k} \frac{4}{xy} dx dy \sup_{x,y \in [0, n/k]} \left| \hat{R}_{i,j,m}(x, y, 1) - \frac{n}{k} C_{i,j,m}(kx/n, ky/n, k/n) \right| + o(1) \\ &= O((\log n)^2) O_{\mathbb{P}}(n^{-\psi}) + o(1) = o_{\mathbb{P}}(1). \end{aligned}$$

Now continuity of $C_{i,j,m}$ together with the dominated convergence theorem imply that for $k/n \rightarrow q \in (0, 1)$ we also have $e_{i,j}^{(m)}(k/n) \rightarrow e_{i,j}^{(m)}(q)$, while for $k/n \rightarrow 0$ this follows from

the arguments given in the proof of Proposition 3. In summary, we have established that for $k/n \rightarrow q \in [0, 1)$ also $\hat{e}_{i,j}^{(m)} = e_{i,j}^{(m)}(q) + o_{\mathbb{P}}(1)$. Combining this with the representations (32), (41) and (60) this shows that $\hat{\Gamma}^{(m)} = \Gamma^{(m)}(q) + o_{\mathbb{P}}(1)$. To complete the proof it thus remains to prove (59).

Proof of (59) We begin with a proof of the following result: for independent observations we have for any $I \subset V, |I| \leq 3$

$$\sup_{\mathbf{x} \in [0,1]^{|I|}} \frac{n}{k} \left| \hat{C}_I(k\mathbf{x}/n) - C_I(k\mathbf{x}/n) \right| = O_{\mathbb{P}}(k^{-1/2}). \quad (61)$$

By the results in Csörgő and Horváth (1987) we have for $j \in V$

$$\sup_{x \in [0,1]} |(n/k)\hat{F}_j^-(kx/n) - x| = O_{\mathbb{P}}(k^{-1/2}).$$

Thus we have with probability tending to one $\hat{\mathbf{F}}^-([0, k/n]^d) \subset [0, 2k/n]^d$, which together with Lipschitz continuity of C with Lipschitz constant 1 implies that with probability tending to one

$$\begin{aligned} & \sup_{\mathbf{x} \in [0,1]^d} \frac{n}{k} \left| \hat{C}(k\mathbf{x}/n) - C(k\mathbf{x}/n) \right| \\ & \leq \sup_{\mathbf{x} \in [0,1]^d} \frac{n}{k} \left| \hat{C}^\circ(\hat{\mathbf{F}}^-(k\mathbf{x}/n)) - C(\hat{\mathbf{F}}^-(k\mathbf{x}/n)) \right| + \sup_{\mathbf{x} \in [0,1]^d} \frac{n}{k} \left| C(\hat{\mathbf{F}}^-(k\mathbf{x}/n)) - C(k\mathbf{x}/n) \right| \\ & \leq \sup_{\mathbf{x} \in [0,2]^d} \frac{n}{k} \left| \hat{C}^\circ(k\mathbf{x}/n) - C(k\mathbf{x}/n) \right| + \sup_{\mathbf{x} \in [0,1]^d} \sum_{j=1}^d \left| \frac{n}{k} \hat{F}_j^-(kx_j/n) - x_j \right| \\ & = \sup_{\mathbf{x} \in [0,2]^d} \frac{n}{k} \left| \hat{C}^\circ(k\mathbf{x}/n) - C(k\mathbf{x}/n) \right| + O_{\mathbb{P}}(k^{-1/2}) \end{aligned}$$

where we recall that the notation \hat{C}° was introduced in (40). Now if $k/n \rightarrow q > 0$, it follows by standard results about the empirical process indexed by rectangles that

$$\sup_{\mathbf{x} \in [0,2]^d} \frac{n}{k} \left| \hat{C}^\circ(k\mathbf{x}/n) - C(k\mathbf{x}/n) \right| = O_{\mathbb{P}}(n^{-1/2}) = O_{\mathbb{P}}(k^{-1/2}).$$

When $k/n \rightarrow 0$ the bound

$$\sup_{\mathbf{x} \in [0,2]^d} \frac{n}{k} \left| \hat{C}^\circ(k\mathbf{x}/n) - C(k\mathbf{x}/n) \right| = O_{\mathbb{P}}(k^{-1/2})$$

follows from corresponding results on the tail empirical process. This completes the proof of (61) and we now continue with the proof of (59). Observe that for $v \geq 1$

$$\frac{n}{k} \{ \hat{C}(k\mathbf{x}/n) - C(k\mathbf{x}/n) \} = v \frac{n}{kv} \{ \hat{C}(kv(\mathbf{x}/v)/n) - C(kv(\mathbf{x}/v)/n) \}.$$

Thus, setting $v = (n/k)^{-\alpha}$, we have for any $1 \geq \alpha > 0$ and any $I \subset V$

$$\sup_{\mathbf{x} \in [0, (n/k)^\alpha]^d} \frac{n}{k} \left| \hat{C}_I(k\mathbf{x}_I/n) - C_I(k\mathbf{x}_I/n) \right| = O_{\mathbb{P}}(k^{-\beta} (n/k)^\alpha). \quad (62)$$

Note in particular that when $k/n^{(1+\kappa)/(1+\beta)}$ is bounded away from zero for some $\beta > \kappa > 0$ we can directly set $\alpha = 1$ and obtain

$$\sup_{\mathbf{x} \in [0, n/k]^d} \frac{n}{k} \left| \hat{C}_I(k\mathbf{x}_I/n) - C_I(k\mathbf{x}_I/n) \right| = O_{\mathbb{P}}(n^{-\kappa}).$$

In particular, this implies that (59) holds in the case $k/n^{(1+\beta/2)/(1+\beta)}$ bounded away from zero in which case we can set $\psi = \beta/2$.

The case $k = o(n^{(1+\beta/2)/(1+\beta)})$ will be discussed next. Observe that for any two functions $f, g : \mathbb{R}^d \rightarrow \mathbb{R}$ which are non-decreasing in every coordinate we have for $\mathbf{a} \leq \mathbf{b}$ (inequalities are interpreted coordinate-wise)

$$\sup_{\mathbf{x} \in [\mathbf{a}, \mathbf{b}]} |f(\mathbf{x}) - g(\mathbf{x})| \leq |g(\mathbf{b}) - g(\mathbf{a})| + |g(\mathbf{b}) - f(\mathbf{b})| + |g(\mathbf{a}) - f(\mathbf{a})|. \quad (63)$$

This follows from a combination of the bounds

$$\begin{aligned} f(\mathbf{x}) - g(\mathbf{x}) &\leq f(\mathbf{b}) - g(\mathbf{a}) = f(\mathbf{b}) - g(\mathbf{b}) + g(\mathbf{b}) - g(\mathbf{a}) \\ f(\mathbf{x}) - g(\mathbf{x}) &\geq f(\mathbf{a}) - g(\mathbf{b}) = f(\mathbf{a}) - g(\mathbf{a}) + g(\mathbf{a}) - g(\mathbf{b}). \end{aligned}$$

For any $\mathbf{x} \in (\mathbb{R}^+)^{|I|}$ define the vectors $\mathbf{v}_{k,n}(\mathbf{x})$ with entries $(\mathbf{v}_{k,n}(\mathbf{x}))_i := n/k$ if $x_i \geq (n/k)^\alpha$ and x_i otherwise and $\mathbf{w}_{k,n}(\mathbf{x})$ with entries ∞ if $x_i \geq (n/k)^\alpha$ and x_i otherwise. With this notation we have for $I = (i_1, i_2, i_3)$, uniformly on $[(n/k)^\alpha, n/k] \times [0, n/k] \times [0, T]$,

$$\begin{aligned} \frac{n}{k} C_I(k\mathbf{v}_{k,n}(\mathbf{x})/n) &\geq \frac{n}{k} C_I(k\mathbf{x}/n) \geq \frac{n}{k} C_I(k(\mathbf{x} \wedge (n/k)^\alpha)/n) \\ &\stackrel{(a)}{=} R_I(\mathbf{x} \wedge (n/k)^\alpha) + O((k/n)^{(1-\alpha)\xi-\alpha}) \\ &\stackrel{(b)}{=} R_I(\mathbf{w}_{k,n}(\mathbf{x})) + O((k/n)^{(1-\alpha)\xi-\alpha} + (k/n)^{\gamma\alpha}) \\ &\stackrel{(c)}{=} \frac{n}{k} C_I(k\mathbf{v}_{k,n}(\mathbf{x})/n) + O((k/n)^{(1-\alpha)\xi-\alpha} + (k/n)^{\gamma\alpha}). \end{aligned}$$

Here (a) follows by (47) applied with $\delta = \alpha, q = n/k$, (b) follows by (52) applied with $\delta = \alpha, q = n/k$ and (c) follows by (47) applied with $\delta = \alpha, q = n/k$ and $I = (i_2, i_3)$ when $x_{i_2} < (n/k)^\alpha$ and holds trivially when $x_{i_2} \geq (n/k)^\alpha$ since in that case $R_I(\mathbf{w}_{k,n}(\mathbf{x})) = x_3 = \frac{n}{k} C_I(k\mathbf{v}_{k,n}(\mathbf{x})/n)$.

In summary, we have proved

$$\sup_{|I|=3} \sup_{\mathbf{x} \in [(n/k)^\alpha, n/k] \times [0, n/k] \times [0, T]} \left| \frac{n}{k} C_I(k\mathbf{v}_{k,n}(\mathbf{x})/n) - \frac{n}{k} C_I(k(\mathbf{x} \wedge (k/n)^\alpha)/n) \right| = O((k/n)^{(1-\alpha)\xi-\alpha} + (k/n)^{\alpha\gamma}) \quad (64)$$

Now for any $\mathbf{x} \in ([0, n/k]^2 \setminus [0, (n/k)^\alpha]^2) \times [0, T]$ apply (63) with $f = \hat{C}_I, g = C_I, \mathbf{a} = k(\mathbf{x} \wedge (n/k)^\alpha)/n, \mathbf{b} = k\mathbf{v}_{k,n}(\mathbf{x})/n$ to obtain for any $|I| = 3$

$$\begin{aligned} &\frac{n}{k} \left| \hat{C}_I(k\mathbf{x}/n) - C_I(k\mathbf{x}/n) \right| \\ &\leq \frac{n}{k} \left| C_I(k\mathbf{v}_{k,n}(\mathbf{x})/n) - C_I(k(\mathbf{x} \wedge (k/n)^\alpha)/n) \right| + \frac{n}{k} \left| \hat{C}_I(k\mathbf{v}_{k,n}(\mathbf{x})/n) - C_I(k\mathbf{v}_{k,n}(\mathbf{x})/n) \right| \\ &\quad + \frac{n}{k} \left| \hat{C}_I(k(\mathbf{x} \wedge (n/k)^\alpha)/n) - C_I(k(\mathbf{x} \wedge (n/k)^\alpha)/n) \right|. \end{aligned}$$

Now by (64) we have (note the supremum in (64) is over all I with $|I| = 3$, so the first two coordinates can be interchanged)

$$\begin{aligned} &\sup_{|I|=3} \sup_{\mathbf{x} \in \{[0, n/k]^2 \setminus [0, (n/k)^\alpha]^2\} \times [0, T]} \frac{n}{k} \left| C_I(k\mathbf{v}_{k,n}(\mathbf{x})/n) - C_I(k(\mathbf{x} \wedge (k/n)^\alpha)/n) \right| \\ &= O((k/n)^{(1-\alpha)\xi-\alpha} + (k/n)^{\alpha\gamma}). \end{aligned}$$

Next, note that by the definition of $\mathbf{v}_{k,n}(\mathbf{x})$ we have

$$\frac{n}{k} \hat{C}_I(k\mathbf{v}_{k,n}(\mathbf{x})/n) = x_3 + O_{\mathbb{P}}(k^{-\beta}) = \frac{n}{k} C_I(k\mathbf{v}_{k,n}(\mathbf{x})/n) + O_{\mathbb{P}}(k^{-\beta})$$

uniformly in $\mathbf{x} \in [(n/k)^\alpha, n/k]^2 \times [0, T]$. Moreover, if $I = (i_1, i_2, i_3)$ then for $\mathbf{x} = (x_1, x_2, x_3) \in [(n/k)^\alpha, n/k] \times [0, (n/k)^\alpha] \times [0, T]$ we have $C_I(\mathbf{x}) = C_{(i_2, i_3)}(x_2, x_3)$ and the same is true for \hat{C}_I . Thus by (62)

$$\begin{aligned} & \sup_{|I|=3} \sup_{\mathbf{x} \in [(n/k)^\alpha, n/k]^2 \times [0, T]} \frac{n}{k} \left| \hat{C}_I(k\mathbf{v}_{k,n}(\mathbf{x})/n) - C_I(k\mathbf{v}_{k,n}(\mathbf{x})/n) \right| \\ & \leq \sup_{|J|=2} \sup_{\mathbf{y} \in [0, (n/k)^\alpha] \times [0, T]} \frac{n}{k} \left| \hat{C}_J(k\mathbf{y}/n) - C_J(k\mathbf{y}/n) \right| \\ & = O_{\mathbb{P}}(k^{-\beta}(n/k)^\alpha). \end{aligned}$$

Combining the arguments above we find

$$\sup_{|I|=3} \sup_{\mathbf{x} \in \{[0, n/k]^2 \setminus [0, (n/k)^\alpha]^2\} \times [0, T]} \frac{n}{k} \left| \hat{C}_I(k\mathbf{v}_{k,n}(\mathbf{x})/n) - C_I(k\mathbf{v}_{k,n}(\mathbf{x})/n) \right| = O_{\mathbb{P}}(k^{-\beta}(n/k)^\alpha + k^{-\beta})$$

Finally, again by (62)

$$\sup_{|I|=3} \sup_{\mathbf{x} \in \{[0, n/k]^2 \setminus [0, (n/k)^\alpha]^2\} \times [0, T]} \frac{n}{k} \left| \hat{C}_I(k(\mathbf{x} \wedge (n/k)^\alpha)/n) - C_I(k(\mathbf{x} \wedge (n/k)^\alpha)/n) \right| = O_{\mathbb{P}}(k^{-\beta}(n/k)^\alpha)$$

Combining the bounds above we obtain

$$\sup_{\mathbf{x} \in [0, n/k]^{|I|-1} \times [0, T]} \left| \frac{n}{k} \hat{C}_I(k\mathbf{x}/n) - \frac{n}{k} C_I(k\mathbf{x}/n) \right| = O_{\mathbb{P}}(k^{-\beta}(n/k)^\alpha) + O((k/n)^{(1-\alpha)\xi-\alpha} + (k/n)^{\alpha\gamma} + k^{-\beta})$$

Now recall that we are in the case

$$n^\theta \leq k \leq n^{(1+\beta/2)/(1+\beta)}$$

where $\theta > 0$ is from the assumptions. Under this assumption we can make α sufficiently small to obtain

$$O_{\mathbb{P}}(k^{-\beta}(n/k)^\alpha) + O((k/n)^{(1-\alpha)\xi-\alpha} + (k/n)^{\alpha\gamma} + k^{-\beta}) = o_{\mathbb{P}}(n^{-\zeta})$$

for some $\zeta > 0$. This completes the proof of (59). \square

S.7.3 Proofs of alternative representations

Proof of (34) and (35) Recall the following representation for the expected value of a non-negative random variable X

$$\mathbb{E}[X] = \int_{[0, \infty)} \mathbb{P}(X > x) dx.$$

The claim in (34) follows by applying this representation to the non-negative random variables $(\log Y_i^m)^\ell \mathbf{1}\{Y_i^m > 1\}$ and $(-\log(Y_i^m))^\ell \mathbf{1}\{Y_i^m \leq 1\}$ and collecting terms. For example

$$\begin{aligned} \mathbb{E}[(\log(Y_i^m))^\ell \mathbf{1}\{Y_i^m > 1\}] &= \int_{[0, \infty)} \mathbb{P}\left((\log(Y_i^m))^\ell \mathbf{1}\{Y_i^m > 1\} > x\right) dx \\ &= \int_{[0, \infty)} \mathbb{P}\left(Y_i^m \mathbf{1}\{Y_i^m > 1\} > \exp(x^{1/\ell})\right) dx \\ &= \int_{[0, \infty)} \mathbb{P}\left(Y_i^m > \exp(x^{1/\ell})\right) dx \\ &= \int_{[0, \infty)} R_{i,m}(\exp(-x^{1/\ell}), 1) dx \\ &= \int_{(0, 1]} \frac{R_{i,m}(x, 1) \ell (-\log x)^{\ell-1}}{x} dx \end{aligned}$$

where the last equality follows with the substitution $u = \exp(-x^{1/\ell})$. Similar arguments show that

$$\begin{aligned}
\mathbb{E}[(-\log(Y_i^m))^\ell \mathbf{1}\{Y_i^m \leq 1\}] &= \int_{[0,\infty)} \mathbb{P}\left((-\log(Y_i^m))^\ell \mathbf{1}\{Y_i^m \leq 1\} > x\right) dx \\
&= \int_{[0,\infty)} \mathbb{P}\left(-\log Y_i^m \mathbf{1}\{Y_i^m \leq 1\} > x^{1/\ell}\right) dx \\
&= \int_{[0,\infty)} \mathbb{P}\left(\log Y_i^m \mathbf{1}\{Y_i^m \leq 1\} < -x^{1/\ell}\right) dx \\
&= \int_{[0,\infty)} \mathbb{P}\left(\log Y_i^m < -x^{1/\ell}\right) dx \\
&= - \int_{[0,\infty)} \mathbb{P}\left(\log Y_i^m \geq -x^{1/\ell}\right) - 1 dx \\
&= - \int_{[0,\infty)} R_{i,m}(\exp(x^{1/\ell}), 1) - 1 dx \\
&= - \int_{[1,\infty)} \frac{(R_{i,m}(x, 1) - 1)\ell(\log x)^{\ell-1}}{x} dx.
\end{aligned}$$

Finally note that

$$\mathbb{E}[(\log Y_i^m)^\ell] = \mathbb{E}[(\log Y_i^m)^\ell \mathbf{1}\{Y_i^m > 1\}] + (-1)^\ell \mathbb{E}[(-\log Y_i^m)^\ell \mathbf{1}\{Y_i^m \leq 1\}]$$

and (34) follows by collecting terms. The claim in (35) follows by similar arguments and details are omitted for the sake of brevity. \square

Proof of (36), (37), (38) and (39) Since the proofs of all statements are similar we only outline the proof of (38). To this end observe that for non-negative random variables X, Y we have

$$\mathbb{E}[XY] = \int_{[0,\infty)^2} \mathbb{P}(X > x, Y > y) dx dy.$$

For a proof, note that

$$\begin{aligned}
\mathbb{E}[XY] &= \int_{\Omega} X(\omega)Y(\omega) d\mathbb{P}(\omega) = \int_{\Omega} \int_{[0,\infty)^2} \mathbf{1}_{(0,X(\omega)) \times (0,Y(\omega))}(x, y) dx dy d\mathbb{P}(\omega) \\
&= \int_{[0,\infty)^2} \int_{\Omega} \mathbf{1}_{(0,X(\omega)) \times (0,Y(\omega))}(x, y) d\mathbb{P}(\omega) dx dy = \int_{[0,\infty)^2} \mathbb{P}(X > x, Y > y) dx dy
\end{aligned}$$

where the order of integration can be interchanged by the Tonelli theorem since the integrand is non-negative. Using this representation and similar computations as in the proof of (34) show that

$$\begin{aligned}
\mathbb{E}[(-\log Y_i^m)(-\log Y_j^m) \mathbf{1}\{Y_i^m \leq 1, Y_j^m \leq 1\}] &= \int_0^1 \int_0^1 \frac{R_{i,j,m}(x, y, 1)}{xy} dx dy \\
\mathbb{E}[(\log Y_i^m)(-\log Y_j^m) \mathbf{1}\{Y_i^m > 1, Y_j^m \leq 1\}] &= - \int_0^1 \int_1^\infty \frac{R_{i,j,m}(x, y, 1) - R_{i,j,m}(\infty, y, 1)}{xy} dx dy \\
\mathbb{E}[(-\log Y_i^m)(\log Y_j^m) \mathbf{1}\{Y_i^m \leq 1, Y_j^m > 1\}] &= - \int_1^\infty \int_0^1 \frac{R_{i,j,m}(x, y, 1) - R_{i,j,m}(x, \infty, 1)}{xy} dx dy
\end{aligned}$$

and

$$\begin{aligned}
&\mathbb{E}[\log Y_i^m \log Y_j^m \mathbf{1}\{Y_i^m > 1, Y_j^m > 1\}] \\
&= \int_1^\infty \int_1^\infty \frac{R_{i,j,m}(x, y, 1) - R_{i,j,m}(\infty, y, 1) - R_{i,j,m}(x, \infty, 1) + R_{i,j,m}(\infty, \infty, 1)}{xy} dx dy.
\end{aligned}$$

Combining those expressions we obtain (38). \square

Proof of (42), (43) and (44) Begin by defining for $I = (i_1, \dots, i_j)$

$$\check{R}_I(\mathbf{x}) := \frac{1}{k} \sum_{t=1}^n I \left\{ \hat{F}_{i_1}(U_{ti_1}) \leq kx_1/n, \dots, \hat{F}_{i_j}(U_{ti_j}) \leq kx_j/n \right\}.$$

We have almost surely

$$\sup_{\mathbf{x} \in [0, n/k]^{|I|}} \left| \hat{R}_I(\mathbf{x}) - \check{R}_I(\mathbf{x}) \right| = O(1/k), \quad (65)$$

this follows for instance from equation (3) in Radulović et al. (2017) and the following discussion.

Next consider any integrable function g with anti-derivative G such that $G(1) = 0$. Then, defining $\hat{U}_{ti} := \hat{F}_i(U_{ti})$ and noting that by definition $1 \geq \hat{U}_{ti} \geq 1/n$,

$$\begin{aligned} \int_{1/k}^1 I \left\{ \hat{U}_{ti} \leq kx/n \right\} g(x) dx &= \int_{[n\hat{U}_{ti}/k, 1 \vee (n\hat{U}_{ti}/k)]} g(x) dx = -G(n\hat{U}_{ti}/k) I \left\{ \hat{U}_{ti} \leq k/n \right\}, \\ \int_1^{n/k} I \left\{ \hat{U}_{ti} > kx/n \right\} g(x) dx &= \int_{[1 \wedge (n\hat{U}_{ti}/k), n\hat{U}_{ti}/k]} g(x) dx = G(n\hat{U}_{ti}/k) I \left\{ \hat{U}_{ti} > k/n \right\}. \end{aligned}$$

Combining the above we find

$$\int_{1/k}^1 I \left\{ \hat{U}_{ti} \leq kx/n \right\} g(x) dx + \int_1^{n/k} \left(I \left\{ \hat{U}_{ti} \leq kx/n \right\} - 1 \right) g(x) dx = -G(n\hat{U}_{ti}/k). \quad (66)$$

To obtain (43) apply this result with $G(x) = (-\log x)^\ell$ to find that

$$\begin{aligned} & \frac{1}{k} \sum_{t=1}^n G \left(\frac{n\hat{F}_i(U_{ti})}{k} \right) I \left\{ \hat{F}_j(U_{tj}) \leq k/n \right\} \\ &= -\frac{1}{k} \sum_{t=1}^n \left(\int_{1/k}^1 I \left\{ \hat{U}_{ti} \leq kx/n \right\} g(x) dx + \int_1^{n/k} \left(I \left\{ \hat{U}_{ti} \leq kx/n \right\} - 1 \right) g(x) dx \right) I \left\{ \hat{F}_j(U_{tj}) \leq k/n \right\} \\ &= -\int_{1/k}^1 \check{R}_{ij}(x, 1) g(x) dx - \int_1^{n/k} (\check{R}_{ij}(x, 1) - 1) g(x) dx \end{aligned}$$

where we used the equality $\sum_{t=1}^n I \left\{ \hat{F}_j(U_{tj}) \leq k/n \right\} = k$ in the last line (note that by independence across t all U_{tj} , $t = 1, \dots, n$ take different values with probability one). Apply the above equality with $G(x) = (-\log x)^\ell$ to obtain

$$\hat{e}_i^{(m), \ell} = \int_{1/k}^1 \frac{\check{R}_{ij}(x, 1) \ell(-\log x)^{\ell-1}}{x} dx + \int_1^{n/k} \frac{(\check{R}_{ij}(x, 1) - 1) \ell(-\log x)^{\ell-1}}{x} dx.$$

Now (43) follows by an application of (65). The proofs of (42) and (44) follow by very similar arguments using the function $G(x) = -\log x$ in (66) and details are omitted for the sake of brevity. \square